TM: Roger G. Norwell

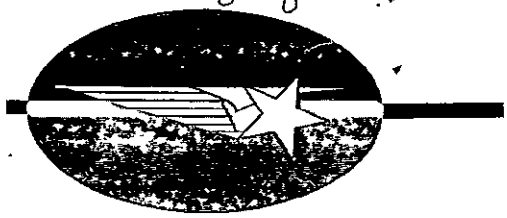

[redacted]

Lockheed

MISSILES & SPACE COMPANY

GROUP DIVISION OF LOCKHEED AIRCRAFT CORPORATION

SUNNYVALE, CALIFORNIA

N-JF-71-1

DEVELOPMENT OF TECHNIQUES AND ASSOCIATED INSTRUMENTATION FOR HIGH TEMPERATURE EMISSIVITY MEASUREMENTS

Contract NAS8-26304

Second Quarterly Progress Report
For the period 30 September 1970 to 31 December 1970

Prepared for

NATIONAL AERONAUTICS AND SPACE ADMINISTRATION
GEORGE C. MARSHALL SPACE FLIGHT CENTER
MARSHALL SPACE FLIGHT CENTER, ALABAMA

Prepared by:

G. R. Cunnington, Project Leader
A. J. Funai, Principal Investigator

Engineering Sciences
Lockheed Palo Alto Research Laboratory
LOCKHEED MISSILES & SPACE COMPANY
A Group Division of Lockheed Aircraft Corporation
Palo Alto, California 94304

FOREWORD

This document was prepared by the Thermophysics Group of the Infrared Programs Laboratory of the Engineering Sciences Directorate, Lockheed Palo Alto Research Laboratory, Lockheed Missiles & Space Company, for the George C. Marshall Space Flight Center of the National Aeronautics and Space Administration. This is the second quarterly report, and it describes the technical activities carried out under Contract NAS8-26304 during the period 30 September 1970 to 31 December 1970. The work was administered under the technical direction of Mr. Roger Harwell, Materials Division, Astronautics Laboratory, Marshall Space Flight Center.

ABSTRACT

Results of studies of the environmental simulation requirements on measurement problems for emittance testing of space shuttle vehicle external surface materials are presented with recommendations for the test conditions. Emittance data for a ceramic coating and an oxidized superalloy (6605) are discussed. Recommendations for the experimental method and apparatus configuration are summarized.

CONTENTS

ILLUSTRATIONS

TABLES

Section 1
INTRODUCTION

Design of thermal protection systems of radiatively cooled vehicles for entry into the earth's atmosphere requires an accurate knowledge of the total hemispherical emittance of the exterior surface material. The advent of the manned, reusable entry vehicle has placed additional requirements on the determination of the radiative properties of candidate materials. Because of the reusability factor, the emittance of these high-temperature materials must be evaluated for repeated exposures to cyclic temperatures in an oxidizing atmosphere at total pressures from less than 1 Torr to nearly atmospheric pressure. Considerations must also be made of the effects of the gas stream in terms of velocity, angle of incidence on the surface, composition, and its temperature in relation to that of the surface, as well as potentially degrading constituents of the ground environment such as water and a humid, salt atmosphere. Measurement of emittance under all of these exposure conditions is a formidable task, and careful attention must be given to the selection of a method or methods of measuring emittance for the various exposure conditions considering both specimen and apparatus costs and accuracy of the data required for thermal design purposes.

A major factor in the selection of the method to be used for measuring emittance is whether the heat transfer parameter of total hemispherical emittance is determined directly or must be computed from total normal or spectral emittance data. If total normal emittance is measured, hemispherical values must be computed assuming a ratio of hemispherical to normal emittance from theoretical considerations or from measured directional data. Spectral data must be treated in a similar fashion with the additional requirement of integration of the spectral data over the blackbody energy distribution for each measurement temperature.

A number of techniques and types of experimental apparatus have been employed for high temperature emittance measurements. Typically, the data obtained in an oxidizing atmosphere have been total normal or spectral normal emittance obtained radiometrically. Total hemispherical emittance data for high-temperature materials have been measured calorimetrically by methods such as a resistively heated strip, tube, or rod; a heat source enclosed within the specimen; or by a decay (transient) method. However, as the calorimetric approach is based upon an energy balance of the specimen with its environment, these measurements generally have been made in vacuum so that radiation is the only significant heat transfer mechanism between the heated specimen and low temperature enclosure or heatsink. Spectral hemispherical reflectance has been measured using arc or solar imaging furnaces, and for opaque bodies the spectral hemispherical emittance is, from Kirchoff's law, equal to one minus the reflectance.

Because of the additional complexity introduced by the environmental simulation aspect, the selection of the optimum technique and the resultant apparatus can be made only after a study of the exposure conditions required to reasonably duplicate the behavior of the radiative properties of the materials under entry conditions. Once this is established, the method most suitable for measurement may be determined. As the type of exposure required for simulation varies with class of material (i.e., super alloy, coated refractory metal, graphite composite, etc.), some tradeoffs will be necessary to evolve an apparatus having maximum flexibility (type of material, nature of radiative properties, etc.), good accuracy, and reasonable cost.

The objective of the program is to develop an experimental method and the apparatus for the measurement of emittance of high temperature materials which may be used in the thermal protection system of the reusable space vehicle measurement goals are:

- Total hemispherical and total normal emittance, from 500° to 3000°F, of refractory metals, superalloys, ceramics, ceramic coatings on electrically conductive substrates, graphites, and carbon composites.
- Measurements are to be made in vacuum of 10^{-5} Torr or in air or oxidizing atmosphere from 10^{-2} to 760 Torr.

- Measurement of total normal emittance during temperature and gas pressure cycling; in addition to a static atmosphere, provisions are to be incorporated for flow of the atmospheric gas over the test area of the specimen during dynamic heating tests.
- Accuracy consistent with requirements for vehicle thermal analysis studies.
- Specimen configuration compatible with current state-of-the-art fabrication capabilities.

The program consists of three phases: the initial portion, Phase I, is a review of the literature and a survey of experimental facilities for high temperature emittance measurements which meet the program goals or may be modified to accomplish these requirements. The activities during this phase are described in Ref. 1 which is the first quarterly progress report for this contract. Phase II is devoted to experimental and analytical investigations of potential measurement problems (temperature, energy, compatibility) and flow simulation requirments for the several classes of materials; selection of the experimental method; design of apparatus and instrumentation; and fabrication and assembly of the apparatus. The results of the first half of this phase are contained in this report. The final phase, Phase III, entails verification testing and delivery and installation of the apparatus at Marshall Space Flight Center.

Section 2

SUMMARY

This report is the second quarterly report to be prepared during the 13-month period of performance of the contract. The activities and accomplishments are described for the initial 3-month period of Phase II of the program. During this reporting period, a study of environmental simulation requirements was completed. On the basis of these results, an analysis of the suitability of existing apparatus for accomplishing these measurement goals was made. Studies of measurement problems were completed, and recommendations for the technique and apparatus design have been prepared.

The results of the simulation requirements study are that supersonic or hypersonic flow conditions are not required for emittance testing of candidate space shuttle vehicle external surface materials. Flow conditions must be such that surface mass transfer rates are similar to or greater than these during entry. This may be accomplished using high subsonic velocity flow. Pressure history must duplicate that experienced during entry. The entry trajectory is such that the boundary layer species concentrations at the surface are identical to air except for the initial phase of flight at the stagnation region. The use of cold gas flows will cause large temperature gradients for materials forming thick oxide layers such as ZrB_2. For this type of material, heated gas should be used to reduce the gradient to a level where composition changes will be similar to those occurring during flight.

Because of the uncertainty in the convective heat transfer coefficient for high velocity flow conditions and the magnitude of this transport mechanism in comparison with the radiative heat transfer, it is not feasible to perform accurate calormetric total hemispherical emittance measurements under these conditions. During flow, total hemispherical emittance will have to be computed from angular emittance data measured radiometrically. For materials which remain stable for a short period of

time, calorimetric total hemispherical emittance can be obtained by interrupting the flow while holding temperature and pressure constant.

The resistance heated strip method offers the most versatility for testing of the candidate materials under flow conditions as radiometric measurements may be performed during flow and calorimetric total hemispherical emittance measurements performed in a static condition. The latter are not feasible using radiant, induction, convection, or furnace heated specimens because of uncertainties in the energy balance. Nonelectrical conductors may be tested by mounting them on a conductive strip or passing it axially through the specimen.

Experimental studies of calormetric measurements with natural convection heat transfer were made to develop corrections to account for this mechanism using a resistively heated strip. Data are presented for oxidized L605 alloy and platinum over the pressure range of 1 to 760 mm Hg. Emittance uncertainties caused by temperature measurement errors introduced by the large gradients in low conductivity coatings were demonstrated experimentally.

Section 3

ENVIRONMENTAL SIMULATION REQUIREMENTS

The radiative properties of high temperature thermal protection system materials for reusable entry vehicles may be significantly altered by repeated exposure to a number of factors of the entry environment. Those most likely to affect these properties are temperature, pressure, velocity, and the composition and temperature of the gas stream in contact with the surface. Temperatures, pressure, and stream composition are parameters which govern chemical reactions and compositional changes that may occur at the surface and coating-to-substrate interface. Shear forces due to the high velocity flows may be of sufficient magnitude to cause removal of portions of surfaces such as oxide films on superalloys or coatings which are at or near their melting temperature. Exposure to these environmental factors takes place during the high temperature segment of the reentry trajectory, and it is during this period that emittance is critical from the temperature control aspect.

Other environmental factors such as vibration, strain, water and salt atmospheres, impact, and abrasion may also play an important role in the performance of the surface material. These, however, will not, in general, be significant during the elevated temperature region of the flight trajectory. Vibrational loads will occur principally during boost and at low altitudes during entry at which times surface temperatures are low. Also, large strains due to aerodynamic forces will not occur in the high temperature portions of the flight. Similarly, exposure to water and salt atmospheres, errosion, and impact, except orbital meteoroid considerations, will be at the low altitude, cooler part of the flight. While these environmental factors are important to the reuse capability, they do not bear directly on emittance stability during a specific entry cycle. As these are very diverse environments from a simulation standpoint, several exposure facilities would probably be required for testing. Specimens could be exposed to these mechanical and low altitude environment conditions and subsequently tested under the simulated emittance measurement entry conditions to evaluate their effects on the radiative behavior of the candidate materials.

In summary, the environmental factors to be examined for emittance studies are temperature, pressure, velocity, and gas composition. The mechanical and low altitude environmental conditions would be investigated using other means, and the radiative properties of materials so exposed could then be evaluated in the proposed apparatus. The effects of these latter factors will not be subject to change with time so that the period between environmental exposure and testing will not bear any influence on the emittance data.

3.1 BOUNDARY LAYER FLOW PROPERTIES

To formulate the entry environment simulation requirements, a study was conducted to develop typical flow properties at several locations on a lifting entry vehicle. The properties important to the materials behavior are temperature, pressure, and concentration of species. By using these calculated data to define the actual environment, estimates may be made of the effect of each boundary layer property on the surface reactions and then the necessity of their simulation in the test apparatus. A Delta body orbiter configuration, Fig. 1, was selected as a representative case for developing an environmental model. This configuration was chosen because of LMSC's extensive studies for this vehicle. Also, significantly higher temperatures would not be expected for the straight wing configuration. The entry trajectory parameters, Fig. 2, were chosen for a 1500-n.m. cross range which results in a longer elevated temperature exposure period. A shorter cross range reduces the exposure time, and it does not increase maximum temperatures except at the stagnation point which may increase by 300°R. Three surface locations representative of maximum temperatures were employed for the analysis; stagnation point, lower surface at mid-body, and the leading edge.

An approximate analysis was carried out to determine temperature, density, and species concentration profiles across the boundary layer. The following assumptions were made for the simplified model:

- Viscous flow field is locally similar in that the boundary layer flow at any point along the vehicle surface approximates a wedge-like local pressure

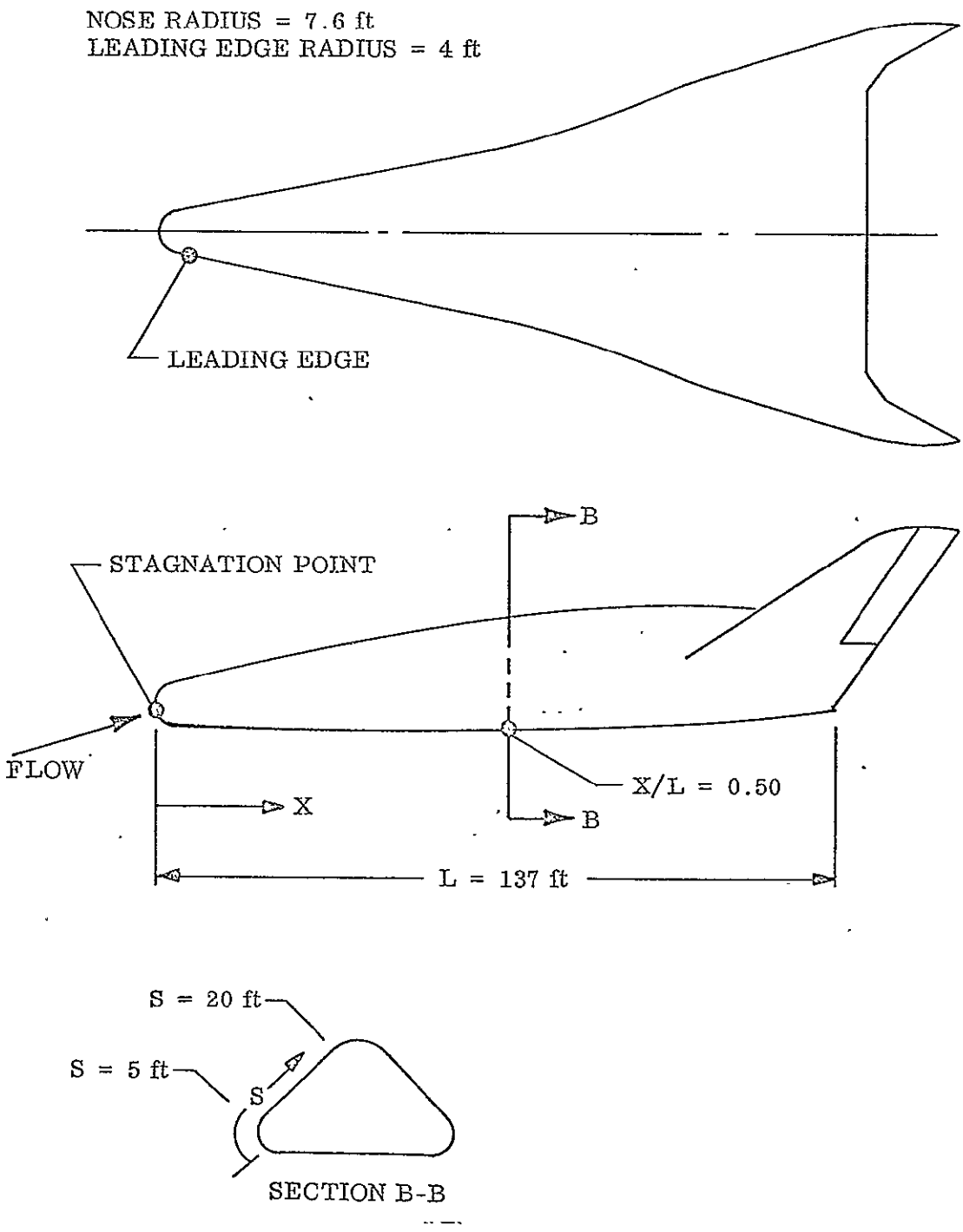

Fig. 1 Delta Body Orbiter Configuration Used for Flow Properties Study

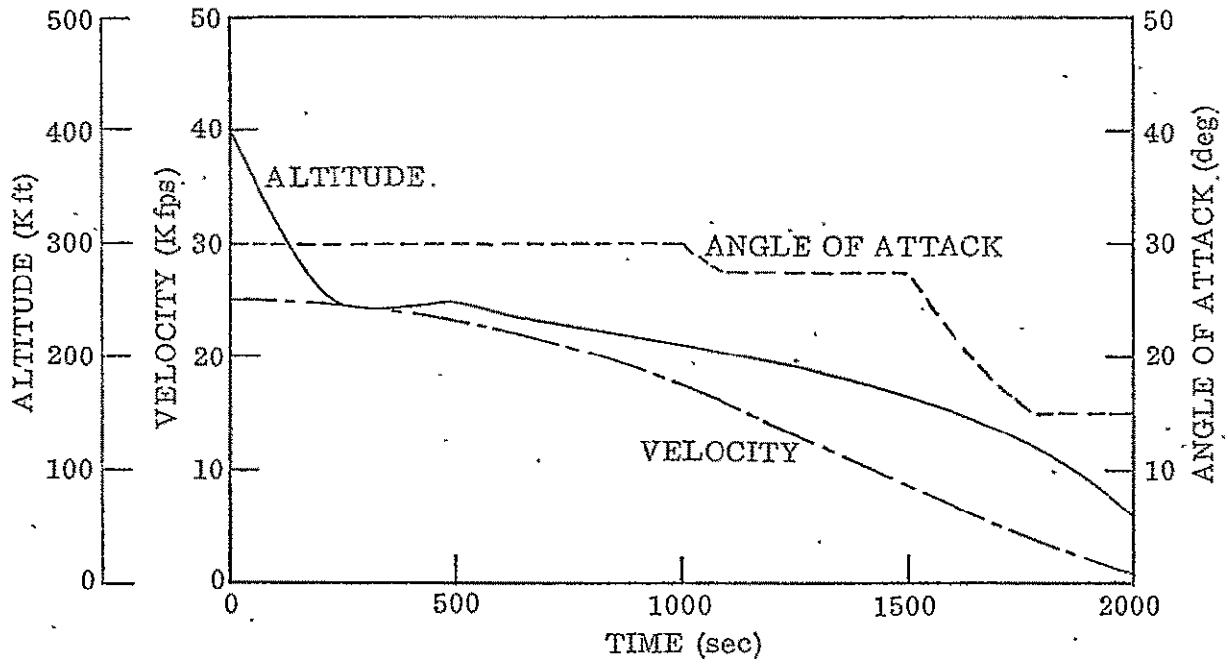

Fig. 2 Typical Delta Body Orbiter Entry Trajectory for a 1500-n.m. Cross Range

gradient. Consequently, a similarity transofrmation can be used to reduce the partial differential equations to the ordinary type for numerical analysis.

- Equilibrium air chemistry with no surface ablation or mass injection.

Using the boundary conditions summarized in Ref. 1, the stagnation-point boundary layer profiles were developed using two functional boundary layer computer programs Vorticity and boundary layer thickness parameters were determined (Ref. 2), and then temperature and density profiles were constructed (Ref. 3). Finally, equilibriun thermochemical calculations were carried out to obtain species concentration profiles

This procedure was also used to compute the boundary layer properties at the lower surface location. However, in contrast to the stagnation point case, laminar-to-turbulent transition occurs at this location during entry. Since the programs are valid only for pure laminar or fully developed turbulent flows, the turbulent option was used when transition was encountered. Also, because of vehicle pitching during entry, crossflow boundary layer effects may occur. However, since this location is on the windward plane of symmetry, a small cross flow is anticipated at moderate angles of attack. Thus, it was neglected for this analysis.

At the leading edge, the swept infinite cylinder theory was used as the vehicle configuration has a relatively straight swept leading edge. For the laminar flow regime, assuming thermochemical equilibrium, the swept cylinder boundary layer profiles of Ref. 4 were used to describe the leading edge case. At lower altitude (< 130 kft), the leading edge flow is turbulent and the 1/5-power low of Ref. 5 was used in profile determination.

Predicted boundary layer profiles for the three locations are presented in Appendix A. Temperature, pressure, density, and species concentration at the surface for the three locations and six altitudes are summarized in Table 1 together with thermodynamic input values used for the analysis. Recommendations for the type of flow simulation required for emittance testing are based upon these data, and they are discussed in the following subsections. Although finite-rate chemistry effects which prevail at high altitudes may invalidate the equilibrium chemistry model for downstream flows, the data generated by this simplified model are considered to be of sufficient accuracy for predicting the order of magnitude of species concentration for this study. A complete boundary-layer/chemical-kinetics analysis would have to be used for more accurate predictions of species concentrations of the midbody and perhaps the leading edge locations.

An analysis of the boundary layer flow properties for a similar shaped but smaller vehicle (Ref. 6) showed that at a point 10-ft aft of the leading edge, the ratio of atomic oxygen recombination time-to-time for diffusion to the wall approached unity. For this condition neither equilibrium nor frozen flow conditions exist, and species concentrations may differ from the equilibrium case. A calculation of species concentrations at the surface for the smaller vehicle at the 10-ft location was performed for a flat plate with a nonequilibrium, turbulent boundary layer (Ref. 7). The assumed trajectory was for superorbital velocity. Boundary layer composition at the plate surface as a function of altitude is shown in Table 2. Comparison of these data with those presented in Table 1 shows that at the surface the equilibrium data agree with the nonequilibrium case except for the initial portion of the trajectory. Because of the relatively low boundary layer temperatures, with the exception of the stagnation region were the equilibrium assumption is valid, the predictions using the simplified analysis are considered to be adequate for defining the simulation environment for emittance testing.

Table 1

THERMODYNAMIC ENVIRONMENT DATA

Time (sec)	Altitude (kft)	M_∞	$\dot{q}$ (Btu/sec-ft^2)	U_e (kft/sec)	P_e (mm Hg)	T_e (°R)	T_w (°R)	δ (ft)	Flow Conditions	Species Concentration at Surface (Mass Fraction)					Density at Surface (lb/ft^3)
										O_2	N_2	O	N	NO	
STAGNATION POINT															
300	244.5	25.4	36	0	19.0	10,550	3000	0.081	Laminar	0.21	0.76	0.02	$<10^{-4}$	10^{-3}	3.3×10^{-4}
1000	207.5	17.3	25	0	47.0	9,600	2865	0.053	Laminar	0.22+	0.76	$<10^{-2}$	$<10^{-4}$	10^{-4}	8.5×10^{-4}
1400	177.5	11.4	8	0	66.7	6,350	2400	0.034	Laminar	0.23	0.76	$<10^{-4}$	$<10^{-4}$	10^{-4}	1.5×10^{-3}
1650	149.3	6.4	3	0	69.6	3,400	1670	0.025	Laminar	0.23	0.76	$<10^{-4}$	$<10^{-4}$	$<10^{-4}$	2.2×10^{-3}
1750	129.7	5.1	—	0	77.8	2,460	1435	0.017	Laminar	0.23	0.76	$<10^{-4}$	$<10^{-4}$	$<10^{-4}$	3.0×10^{-3}
1850	103.6	3.9	—	0	84.7	1,680	1175	0.010	Laminar	0.23	0.76	$<10^{-4}$	$<10^{-4}$	$<10^{-4}$	4.0×10^{-3}
LOWER SURFACE AT X/L = 0.5															
300	244.5	25.4	6	19.9	5.0	6,300	1900	0.397	Laminar	0.23	0.76	$<10^{-4}$	$<10^{-4}$	10^{-3}	1.4×10^{-4}
1000	207.5	17.3	15	14.6	12.8	5,350	2660	4.17	Turbulent	0.23	0.76	10^{-3}	$<10^{-4}$	10^{-3}	2.5×10^{-4}
1400	177.5	11.4	5	10.3	14.9	3,360	2160	3.44	Turbulent	0.23	0.76	$<10^{-4}$	$<10^{-4}$	10^{-3}	3.6×10^{-4}
1650	149.3	6.4	2	6.0	15.7	1,400	2100	1.17	Turbulent	0.23	0.76	$<10^{-4}$	$<10^{-4}$	10^{-3}	3.9×10^{-4}
1750	129.7	5.1	—	4.7	17.7	920	1500	0.294	Turbulent	0.23	0.76	$<10^{-4}$	$<10^{-4}$	10^{-3}	6.0×10^{-4}
1850	103.6	3.9	—	3.6	22.5	580	1115	0.0325	Turbulent	0.23	0.76	$<10^{-4}$	$<10^{-4}$	10^{-3}	1.1×10^{-3}
LEADING EDGE															
300	244.5	25.4	14	20.2	5.8	6,250	2380	0.166	Laminar	0.23	0.76	$<10^{-4}$	$<10^{-4}$	10^{-3}	1.3×10^{-4}
1000	207.5	17.3	10	15.0	13.3	4,920	2290	0.091	Laminar	0.23	0.76	$<10^{-4}$	$<10^{-4}$	10^{-4}	3.0×10^{-4}
1400	177.5	11.4	3	10.8	15.5	2,870	1880	0.058	Laminar	0.23	0.76	$<10^{-4}$	$<10^{-4}$	10^{-4}	4.3×10^{-4}
1650	149.3	6.4	1	6.2	15.1	1,250	1325	0.047	Laminar	0.23	0.76	$<10^{-4}$	$<10^{-4}$	10^{-4}	6.0×10^{-4}
1750	129.7	5.1	—	4.8	16.0	890	1425	0.035	Turbulent	0.23	0.76	$<10^{-4}$	$<10^{-4}$	10^{-4}	5.9×10^{-4}
1850	103.6	3.9	—	3.6	18.7	610	1145	0.026	Turbulent	0.23	0.76	$<10^{-4}$	$<10^{-4}$	10^{-4}	8.5×10^{-4}

Notes: M_∞ is freestream Mach number.

δ is boundary layer thickness.

Subscripts e and w refer to outer edge and wall conditions, respectively.

Table 2

NONEQUILIBRIUM SURFACE SPECIES CONCENTRATIONS

Time (sec)	Altitude (kft)	U_e (kft/sec)	P_e (mm Hg)	T_w (°R)	Species Concentration at Wall O_2	O	N_2
300	226	31.2	5.4	2530	0	0.23	0.76
600	226	26.6	3.9	2160	0.20	0.03	0.76
900	226	23.2	3.0	1870	0.22	0.01	0.76
1200	226	20.5	2.3	1700	0.23	0	0.76
1800	207	16.1	3.1	1460	0.23	0	0.76

3.2 VELOCITY SIMULATION

Boundary layer velocity conditions may contribute to the radiative performance of the surface material in terms of shear forces and mass transfer. Although no facility exists for exact simulation of the velocity and pressure conditions encountered during the entry trajectory, the requirement of approximating this environment by using supersonic or hypersonic flow conditions is examined. Consider first the mechanical effects of shear stresses at the wall. These may cause the thinning or total removal of a semiliquid or liquid surface layer or a loosely adhering solid oxide film. As long as a glassy like material is used at a temperature sufficiently below its melting or softening temperature, simulation of shear forces is not necessary as demonstrated by the oxidation performance data of Perkins and Packer (Ref. 6). They exposed coated TZM (99 Mo-Ti-Zr) specimens to flow at various specimen temperatures in a Mach 3 turbulent duct. At temperatures below 2900°F for pressures of 5 and 20 mm Hg, they noted essentially no difference in useful life from those observed for slowly moving air tests. Similar agreement is reported for coated columbium-based alloys and a Sn-Al coating on Ta-10 W. Although thinning of the coating occurred for the latter material, oxidation resistance was not significantly altered from low velocity tests.

If the surface layer is homogeneous and has a very large extinction coefficient, such as a metal, emittance at elevated temperatures may be considered to be independent of thickness once an opaque layer is achieved. However, this may not hold for some of the glassy like materials, and the composition as a function of depth may change during exposure. Consequently, stability of radiative properties can not be related to oxidation performance for all materials. No quantitative data have been found in the literature which relates emittance to flow conditions. Kaufman et al. (Refs. 8 and 9) report emittance data from supersonic arc and subsonic test facilities for a number of materials. However, no conclusions can be drawn regarding velocity effects because low velocity tests were conducted at nearly atmospheric pressures, whereas supersonic flow conditions were achieved at much lower pressures. Goldstein and Centalanzi (Ref. 10) have studied several Td-Nr-Cr alloys in a supersonic arc tunnel. They observed differences in visual appearance of the surface between tunnel tests and the preoxidized material (furnace). However, only limited emittance data were obtained ($\lambda \approx 0.65\mu$), and no comparison was presented regarding different flow conditions.

Another important factor of velocity is its effect on the mass transfer parameter at the surface. For emittance testing, the conditions should be such that the reactions in this test environment proceed as they would in the entry environment. If this condition is met, then the surface composition and radiative properties should be the same as for flight conditions. For a material or surface for which the reaction kinetcs are known, the mass transfer at the wall may be related to the heat transfer coefficient (Stanton Number) and the velocity and density, evaluated at boundary layer edge conditions. Thus, flow properties may be adjusted so as to result in the mass transfer which is calculated for the specific material under flight conditions.

As discussed earlier, no data were found in the literature on flow velocity (i.e., subsonic or supersonic) effects on emittance of potential reusable materials. There are, however, data on oxidation behavior for both types of flows for several materials Boeing (Ref. 11) did a study on the oxidation of uncoated molybdenum. They computed the attack rate for the X-20 vehicle environment for various pressures and temperatures. The experimental data were obtained from a series of tests using near sonic

flow of low temperature air over a resistance heated strip of molybdenum. Their results showed that the lower velocity conditions gave rates comparable to the values predicted for the flight environment.

Buckley et al. (Ref. 12) presented recession rate data for ATJ graphite and several graphite composites from both subsonic and supersonic arc tunnel data. Surface temperatures were on the order of 4000°F for the former and 4900°F for the latter test conditions. The ATJ recession rates did not increase greatly for supersonic flow. The JTA composite showed a large increase in recession rate by going to supersonic conditions, but the author indicated that this was probably due to the higher temperature, and velocity was a small effect. Data reported by Kaufman et al. (ref. 8) for a number of materials show that at temperatures of 3000°F or less no significant differences in recession rates were observed between supersonic and high velocity subsonic flows.

Based upon these recession rate studies, supersonic flow conditions are not necessary to achieve the mass transfer rates which will adequately simulate the shuttle vehicle entry conditions. Considering that the candidate materials are selected for long-term stability in order to have a reuse capability of 100 cycles, their reaction rates with the oxidizing atmosphere will be much less than the bare refractory metal or graphite. Consequently, the mass flow associated with the near sonic velocity at the specimen will provide adequate mass transfer for these materials so that reactions will not be diffusion limited (oxygen in the boundary layer).

3.3 PRESSURE SIMULATION

Simulation of the entry pressure history at the surface of the material is necessary. The partial pressures of the gas species participating in the reaction and the total pressure are major parameters in the reaction and mass transfer rates. The test apparatus therefore, should have the capability of simulating the pressure cycles at various locations on the vehicle. (See Table 1.) Also, the high temperature oxidation performance of some materials degrades at pressures less than 1 mm Hg

(Ref. 6), and some of the interior surfaces of the vehicle will be exposed to these very low static pressures during peak heating. Consequently, the apparatus should have the capability of achieving pressures as low as 10^{-3} mm Hg.

3.4 COMPOSITION SIMULATION

As discussed in subsection 3.1, the composition at the surface is that of air except in the stagnation region for the initial portion of the trajectory. Although no data were found in the literature regarding reactions with dissociated oxygen, it is believed that the short elevated temperature exposure to atomic oxygen will not have a significant effect on the radiative behavior of the candidate materials (Ref. 6).

3.5 TEMPERATURE SIMULATION

The principal area in question concerning the requirements for gas temperature simulation is that of the thermal gradients across the surface layer. In actual flight, the exterior surface is at a higher temperature than the substrate. For materials that form thick, relatively low thermal conductivity oxide layers, very large gradients will exist between the substrate and the surface. For hot-gas plasma arc tests, Kaufman et al. (Ref. 9) report large gradients, on the order of 50°F/mil, for ZrB_2 in the temperature range of 4000° to 4500°F. Conversely, for cold gas flow conditions at low flow velocity, 50 ft/sec, and 3400°F substrate temperature, the gradient was on the order of 15° to 20°F/mil of oxide (surface temperature lower than substrate). If cold gas is used for testing of materials which form a thick oxide layer, such as ZrB_2, surface temperatures may be as much as 200° to 400°F lower than the substrate temperature at a surface temperature of 3000°R.

Materials which form a thinner oxide layer, such as on the superalloys or a coated refractory metal, will not be subject to such large gradients. Estimates of the gradient per mil of coating or oxide thickness have been calculated for radiative only and convective plus radiative heat transfer (cold gas) as a function of surface temperature, and they are shown in Fig. 3. A thermal conductivity of 1.0 Btu/hr-ft-°F, which

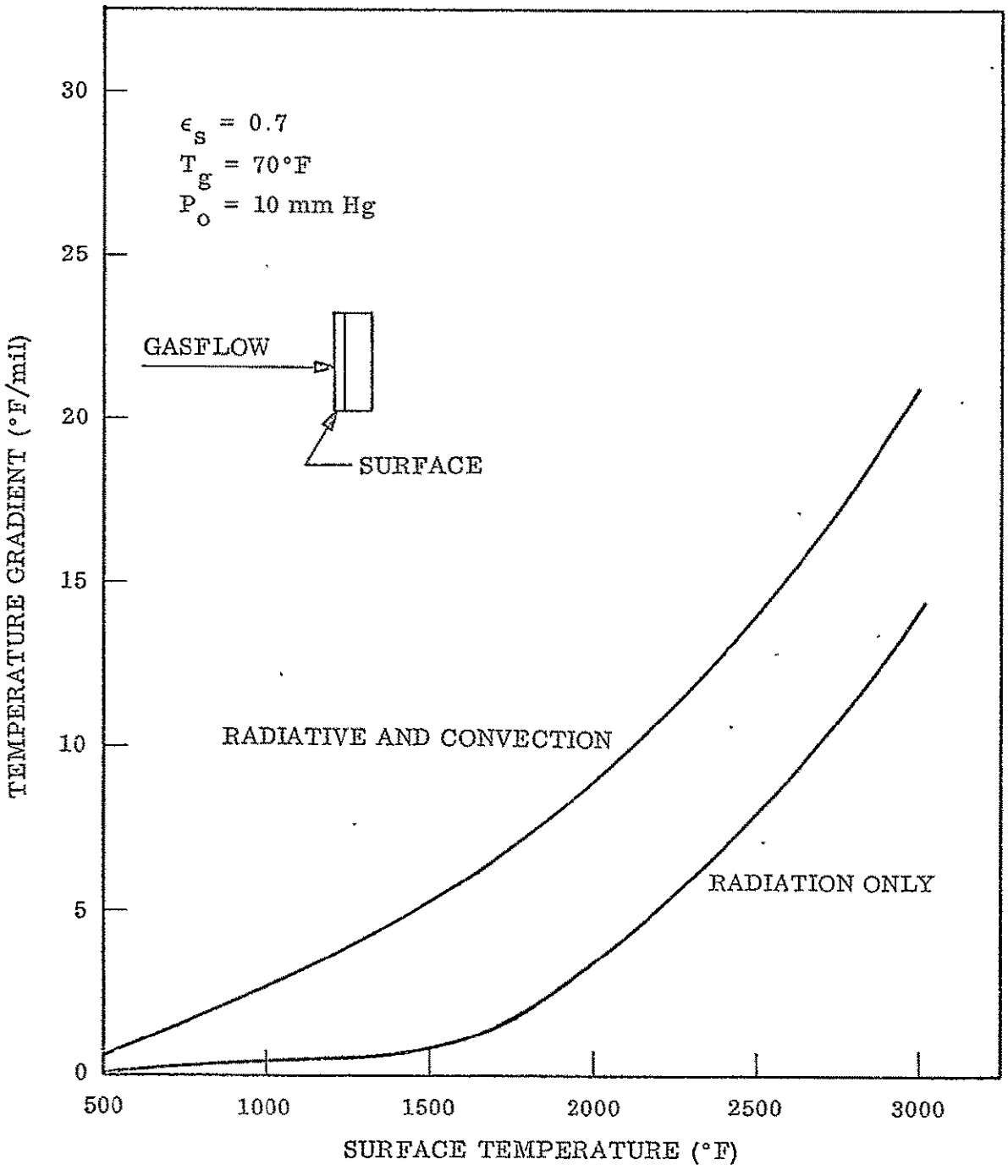

Fig. 3 Temperature Gradient per mil of Thickness for a Glass-Like Coating for Heated Substrate Conditions

is typical for glassy like material, was used for these calculations. For a heated substrate case and a 3000°F surface temperature with a 5-mil thick coating, the substrate temperature would be 3070°F for radiation losses only, and 3110°F for radiative plus convective losses due to the near sonic flow normal to flat plate speciment. Conditions for the super alloys which form thin oxide layers (on the order of 1 mil) at 2000°F result in negligible gradients, 5° to 10°F.

For testing of materials that form thick layers of low thermal conductivity material, such as the diborides, the use of a cold gas flow will result in large temperature differences between substrate and surface which may influence the reactions occurring at the interface and in depth in the surface layer. For these materials it would be desirable to use a hot gas flow so that the gradients may be minimized, approximately 100°F for the 3000°F maximum temperature conditions. For coated refractory metals, graphites, and superalloys, the use of a cold gas flow should not produce temperature gradients which will significantly affect the material behavior.

3.6 RECOMMENDED SIMULATION CONDITIONS

In summary, the simulation conditions recommended for emittance testing of the candidate materials, are as follows:

- Supersonic flow not required, near sonic velocity conditions are adequate to assure that mass transfer rates are comparable to those under entry conditions.
- Pressure history to follow entry environment conditions for various body locations.
- Cold gas acceptable for coated refractory and superalloy materials, hot gas desirable for materials which form thick oxide scales.

The apparatus design also should be such that emittance measurements may be made on post exposure specimens tested under conditions of high shear forces, such as in a supersonic facility, or under mechanical environmental exposures simulating impact, errosion, strain, etc.

Section 4
ANALYSIS OF EXISTING APPARATUS

The results of the survey of current emittance test facilities are discussed in Ref. 1, and the various types of apparatus are listed in tabular form in Table 3. None are currently setup to accomplish all of the measurement goals of the program. Of those which give a reasonable simulation of the entry environment, none are equpped for total hemispherical emittance measurement. Brief summaries of each of the basic types of facilities are given in the following paragraphs.

- Plasma-Arc Tunnel. This type most nearly simulates entry conditions in that supersonic velocites are achieved, Mach numbers of 2 to 5, and the stream temperature is greater than surface temperature. At pressures corresponding to the entry trajectory surface, shear stresses and velocity are much lower than for flight. The specimen temperature and pressure profiels can be simulated for the time periods corresponding to the range of shuttle vehicle trajectories. Stagnation, inclined plate, wedge, and wall (turbulent duct) flow conditions can be obtained. This type of apparatus could be modified for total and spectral normal and angular emittance measurements. However, the uncertainties in the energy balance on the specimen will result in poor accuracy of total emittance measurements during flow. Although the specimen is convectively heated, data could possible be obtained for no flow conditions from a transient analysis, but again the thermal balance uncertainties will result in poor accuracy for the value of ϵ_{TH}.

- Resistance Heating. The resistance heated strip method used by Boeing (Ref. 13) for the X-20 program studies was reported to satisfy the mass transfer rate criteria for coated refractory metals. This apparatus used a near sonic velocity free jet of ambient air impinging on the central area of the specimen to achieve the necessary mass transfer. The apparatus can duplicate the pressure and temperature requirements of the shuttle vehicle trajectories. The apparatus was instrumental for total normal and spectral (0.65μ) normal emittance measurements

Table 3

SUMMARY OF EMITTANCE TEST FACILITIES FOR MEASUREMENTS IN AIR AT ELEVATED TEMPERATURES

Facility	Radiative Property	Specimen Heating	Pressure Range	Flow Simulation	Comments
(1) AVCO Corporation Wilmington, Mass.	$\epsilon_\lambda(0.65\ \mu m)$ ϵ_{TN}	Plasma-arc tunnel	Vacuum to 1 atmosphere	Supersonic flow, simulates 90% of stagnation enthalpy and pressure range	Continous run time of 60 min., hot gas flow; possibility of sample contamination from arc.
(2) Arthur D. Little, Inc. Cambridge, Mass.	$\rho_\lambda(\epsilon_\lambda)$	Arc-imaging furnace and induction heated specimen	Atmospheric pressure Vacuum to 1 atmosphere	Static air or other gases inert gases	Possibility of specimen contamination of optics.
(3) Boeing Company Kent, Wash.	$\epsilon_\lambda(0.65\ \mu m)$ ϵ_{TN}	Sample resistance	Vacuum to 1 atmosphere	Air or other gases, sonic nozzle at fixed angle with respect to test surface	Continuous run can duplicate cyclic temperature and pressure requirements; flow reported to be adequate simulation for silicide-coated refractory metal.
(4) Grumman Aerospace Corporation Bethpage, Long Island, N.Y.	$\epsilon_\lambda(0.65\ \mu m)$ ϵ_{TN} ϵ_{TH}	Sample resistance	Vacuum to 1 atmosphere	Static air or other gases	No flow simulation capability
(5) IIT Research Inst. Chicago, Ill.	$\epsilon_\lambda(1$ to 14 μm and $0.65\ \mu m)$ ϵ_{TN}	Furnace	Atmospheric	Static air or other gases	No flow simulation capability.
(6) LTV Aerospace Corporation Dallas, Tex.	ϵ_{TN}	Gas and plasma torches impinging in specimen faces	Atmospheric	N_2 or N_2/O_2 mixture for plasma torch mixed with ambient air, subsonic velocity	No capability for pressure variation.
(7) Lockheed Missiles & Space Company Palo Alto, Calif.	$\epsilon_\lambda(0.65\ \mu m)$	Induction heated	Atmospheric	Static to 250 fps air or other gases	No capability to cover pressure range; low to accelerate flow velocities.
	$\epsilon_\lambda(0.4$ to 25 $\mu m)$ ϵ_{TN} ϵ_{TH} (angular data for ϵ_λ and ϵ_T from 0° to ±88° from normal; also polarizers)	Specimen resistance	Vacuum to 1 atmosphere	Static air or other gases	No flow simulation capability.
(8) Material Consultants, Inc. Denver, Colo.	$\epsilon_\lambda(0.65\ \mu m)$ ϵ_{TN} ϵ_{TH}	Sample resistance	Vacuum to 1 atmosphere	Static air or other gases	No flow simulation capability.
(9) McDonnell Douglas Corporation St. Louis, Mo.	$\epsilon_\lambda(1$ to 14 μm and $0.65\ \mu m)$ ϵ_{TN}	Induction heated	Vacuum to 1 atmosphere	Static and very low velocity air or other gases	No moderate to high velocity flow simulation.
(10) North American Rockwell Los Angeles, Calif.	$\epsilon_\lambda(1$ to 14 μm and $0.65\ \mu m)$ ϵ_{TN}	Furnace	Vacuum to 1 atmosphere	Static and very low velocity air or other gases	No moderate to high velocity flow simulation
(11) Pratt & Whitney Aircraft East Hartford, Conn.	ϵ_λ ϵ_{TN} ϵ_{TH}	Specimen resistance	Vacuum to 1 atmosphere	Static and very low velocity air or other gases	No moderate to high velocity flow simulation.
(12) Southern Research Inst. Birmingham, Ala.	$\epsilon_\lambda(0.65\ \mu m)$ ϵ_{TN}	Induction heating	Vacuum to 1 atmosphere	Static air or other gases	No flow simulation capability.
(13) Plasma Arc Facilities (ref)Tunnels at NASA, LRC and ARC, Martin Marietta/Baltimore, Aerotherm and Plasmadyne	ϵ_λ from optical pyrometer or visible/near IR radiometer	Plasma-arc tunnel	Vacuum to near atmosphere pressure	Supersonic flow; various facilities simulate stagnation enthalpy and pressure from 70% to 100% of desired range.	Facilities not setup for total or spectral (over sufficiently wide-band) for emittance studies, possibility of sample contamination from arc.

during flow. It could be modified for angular and a wider range of spectral data as well as to perform calorimetric total hemispherical emittance measurements with the flow interrupted. Various flow angles may be obtained by moving the nozzle or rotating the specimen plane.

None of the other facilities employing the heated strip or filament heating method are equipped for simulation of flow conditions. They, however, could be modified to accomplish the same performance as the Boeing apparatus. Principally, this would entail the addition of instrumentation and a nozzle with the pumping system to accommodate the high mass flows at the low pressures.

- Induction Heating. Facilities using induction heating of the specimens could also be modified to incorporate means for high velocity flow, pressure simulation, and radiometric emittance measurement capabilities similar to those discussed previously. Total hemispherical emittance cannot be measured directly because of the difficulty in evaluating the power input from an energy balance during heating. For the transient condition, the problems are similar to those in an arc tunnel. One problem associated with induction heating is the requirement for a susceptor material for nonconductors or thin sheet specimens which will survive the test environment. For flow tests, the specimen surface must be flush with the face of the susceptor, and for thin samples it is difficult to obtain a uniform temperature distribution over the test area.

- Furnace. This type of heating method is not suitable for the dynamic conditions becuase of the poor cyclic temperature response of a furnace and the difficulty in achieving high velocity flow in the furnace hot zone while maintaining the advantage of near blackbody conditions which minimizes the specimen temperature measurement problem. Also, total hemispherical emittance measurements cannot be performed under these conditions and in general, angular measurements cannot be made because of the constructional features of a furnace.

The two concepts of apparatus which can be modified to meet the majority of the measurement objectives are the plasma arc and the resistance (Boeing) facilities. Considering that supersonic flow is not required, as discussed in Section 3, the latter type of apparatus is recommended over the plasma arc for the following reasons:

- Adaptable to direct measurement of total hemispherical emittance
- Pressure simulation from $< 10^{-4}$ to 760 mm Hg
- Suitable for low temperature range (300° to 1000°F) material studies
- No problem of contamination of specimen surface by environment, i.e., arc
- Configuration more adaptable to radiometric instrumentation

Therefore, it is recommended that the program proceed toward the development and fabrication of an apparatus similar to that used by Boeing, including modifications for heating of the gas stream, heating of electrically nonconducting specimens, and instrumentation for total hemispherical emittance and additional radiometric-emittance measurements.

Section 5

APPARATUS DEVELOPMENT AND FABRICATION PLAN

The basic apparatus concept selected for this program is to use a resistivity heated specimen mounted in a water cooled chamber in which the ambient pressure may be varied from 10^{-4} to 760 mm Hg. A near sonic velocity flow of air is directed onto the specimen at fixed angles of incidence to simulate the entry environment mass transfer rates. Specimen temperature and pressure can be varied with time to simulate those occurring during entry at various locations on the vehicle surface. Instrumentation is tobe provided for measurement of surface and substrate temperature and total and spectral normal and total angular emittance during cyclic tests with flow directed onto the specimen. Capability for calorimetric total hemispherical emittance measurement under static conditions will also be incorporated into the facility. Finally, consideration will be given to the feasibility of providing a hot gas system.

The spectral emittance measurement capability is desirable for several reasons. One, this type of data is of great assistance in interpreting observed variations in total emittance due to temperature or to compositional changes in a material with temperature and/or pressure cycling. Second, spectral data may be used to assist in radiometric determinations of surface temperature for nongray materials. From a knowledge of the relative spectral emittance in the infrared region, several wavelengths may be selected such that their spectral emittance values are nearly equal, and the two-color methos then utilized to improve temperature measurement accuracy. Last, spectral data are required for heat transfer analysis between nongray surfaces at widely differing temperatures.

The feasibility of incorporating into the apparatus a system for heating the gas must be considered further in terms of the cost and increased control problems for the cyclic testing. As discussed earlier, large temperature gradients will be present in materials which form a thick, relatively low thermal conductivity surface layer

during exposure. Also, this gradient will change with time as the layer thickness increases. If cyclic testing is to be conducted with surface temperature as the controlling parameter, the substrate temperature will then be considerably higher because of the high surface heat fluxes from radiation and convections. These losses can be reduced significantly by heating the gas stream to a temperature higher than the surface so that the convective energy added to the surface compensates for the loss by radiation. This type of simulation is probably important only for the portion of the cycle at higher temperature, i.e., greater than 2000°F. At temperatures below this, the gradients will be less, and the probability of compositional changes in the coating and substrate will be much less for these refractory type materials. A tradeoff study will be made considering added cost because of the heating unit (possibly an r-f plasma) and flow ducting, increased control complexity for cyclic operation and the number of materials of this type which are considered as strong candidates for use on the space shuttle vehicle. The best choice at this time may be to construct the apparatus so that this capability could be added at a later date if needed.

5.1 DEVELOPMENT AND FABRICATION PLAN

Figure 4 diagrammatically shows the sequence of developmental, fabrication, assembly and checkout operations to be performed in preparing the completed test facility. The initial portion of Phase IIa involves the preparation of the finalized basic apparatus design ;drawings and equipment specifications. Concurrent with this will be a component development and design effort. This will cover optimization of the flow nozzle for uniformity of mass flow and pressure at the specimen test area, design of the radiometric and optical instrumentation, finalization of the clamping fixture for maintaining uniform loading under the cyclic temperature variations, and the study of the heated gas feature.

Preliminary studies indicate that a simple convergent nozzle will be adequate for stagnation conditions. At chamber pressures below 400 mm Hg, the velocity is sonic at the throat and the nozzle is a constant mass flow device. Over the central specimen area, corresponding to one-half of the stip width, the pressure will be

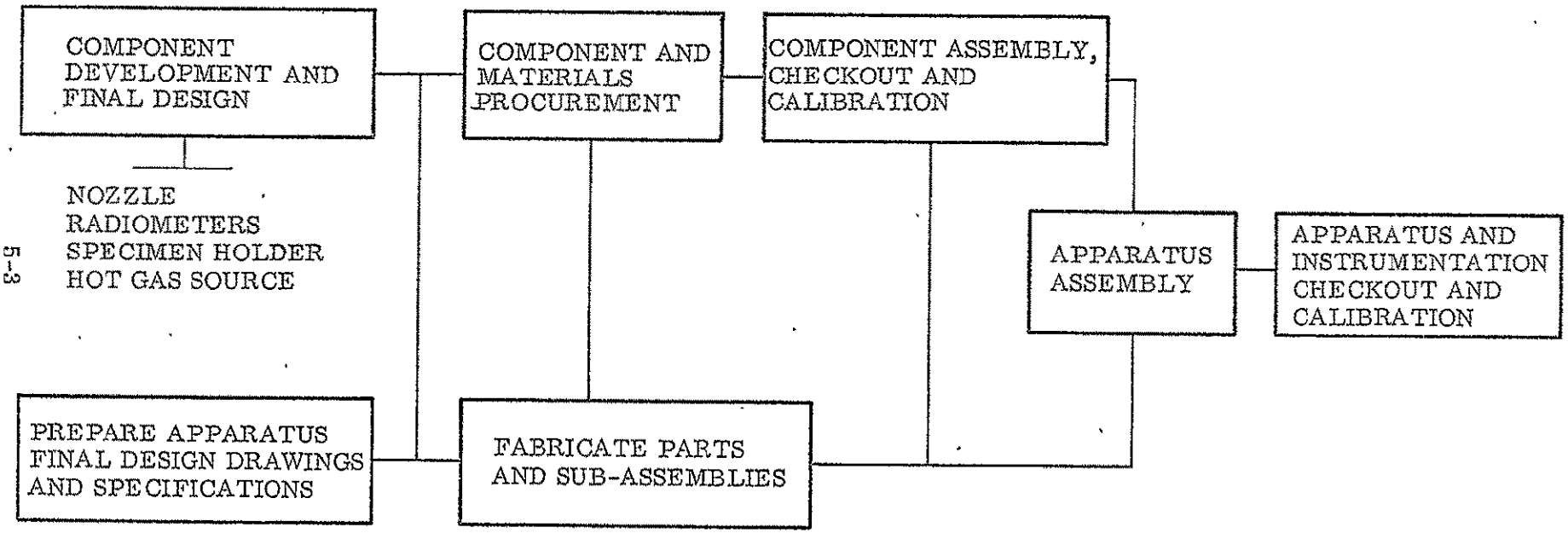

Fig. 4 Phase IIa Apparatus Development, Fabrication, and Checkout Plan

uniform and equal to approximately 2.5 times chamber pressure. However, further study has to be made of the mass flow distribution. Velocity would be near sonic as the specimen would be located downstream of the base shock in the free jet. Boeing (Ref. 13) utilized this arrangement for their testing, and the nozzle throat size was such that the flow could be handled by a 1200 cfm pump over the desired pressure range. An alternate approach is to use a large nozzle diameter and operate subcritically so that more uniform flow is obtained at the specimen. This requires an upstream reservoir at a pressure equal to the desired specimen stagnation pressure, and the larger nozzle size blocks more of the specimen area from viewing in a near normal direction by the radiometric instrumentation.

Radiometric development will be devoted principally to the selection of the optical system for viewing the specimen, and the means for obtaining spectral data. A focused system offers the advantage of collecting a larger amount of energy for spectral and lower temperature measurements. However, as it is an imaging system, it is subject to effects of local nonuniformities in surface temperature and variations of detectors sensitivity over the illuminated area. A collimated optical design eliminates these problems as it is "averaging" in the sense that each bundle of rays fills the detector. Its disadvantage is that it collects a smaller amount of energy and therefore, requires a better detector/amplifier system for spectral and low temperature measurements.

Considering cost and rapidity of operation, it is recommended that spectral data be obtained over the 1.0- to 10-μ region using a narrowband filter wheel device. As most of the materials to be investigated do not show a large amount of band structure, a continuous spectrum is not necessary. Intervals of 1 μ will be adequate to describe the spectral characteristics of most of the candidate materials.

5.2 APPARATUS

The proposed apparatus layout is shown in Figs. 5 and 6. The specimen is held between water-cooled electrode clamps, one of which is self-compensating for expansion and contraction of the specimen during the cycling heating. Electrical power for heating is supplied from a 10 kVA, low voltage ac supplied through water

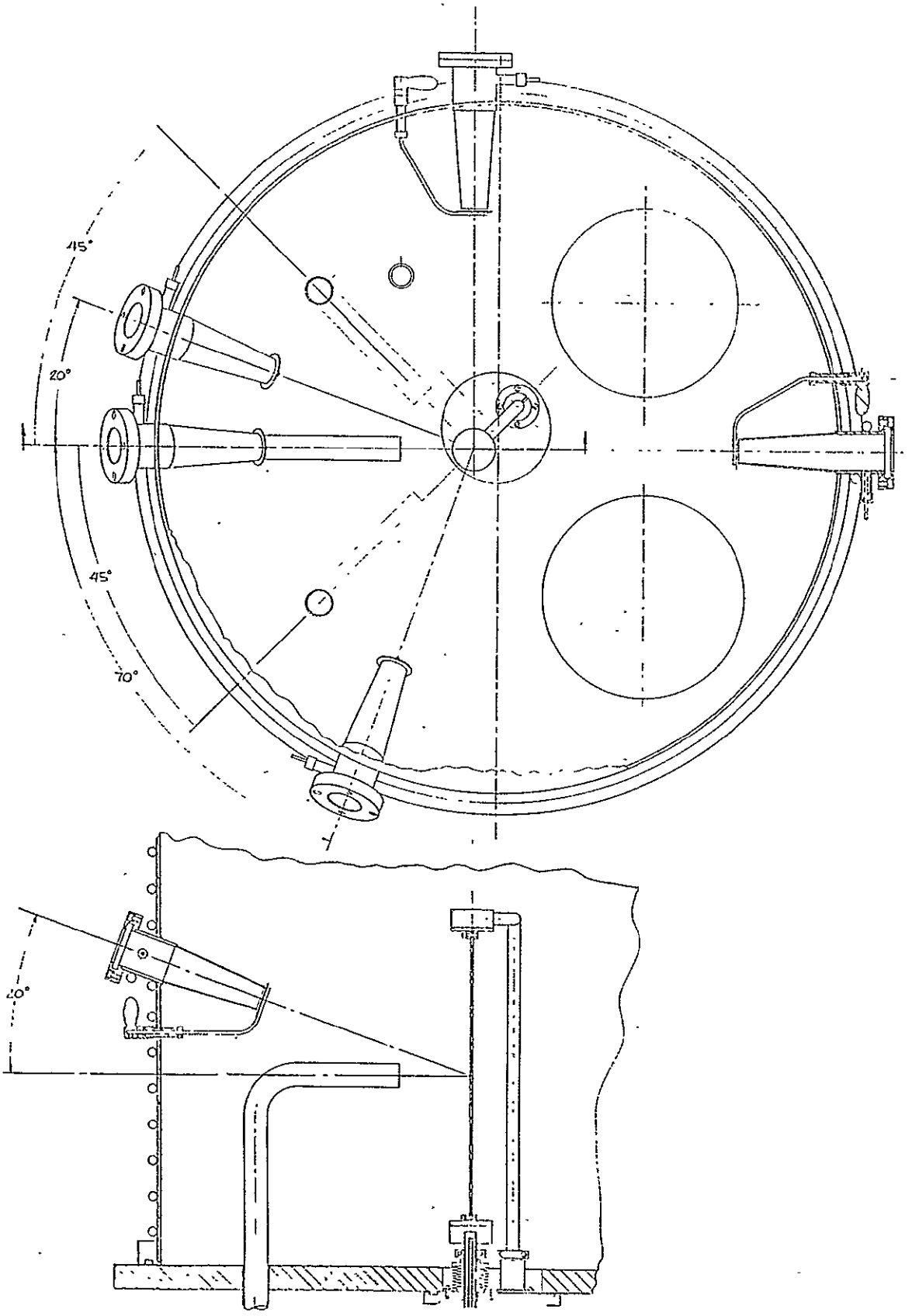

Fig. 5 Chamber Layout of High Temperature Emittance Apparatus

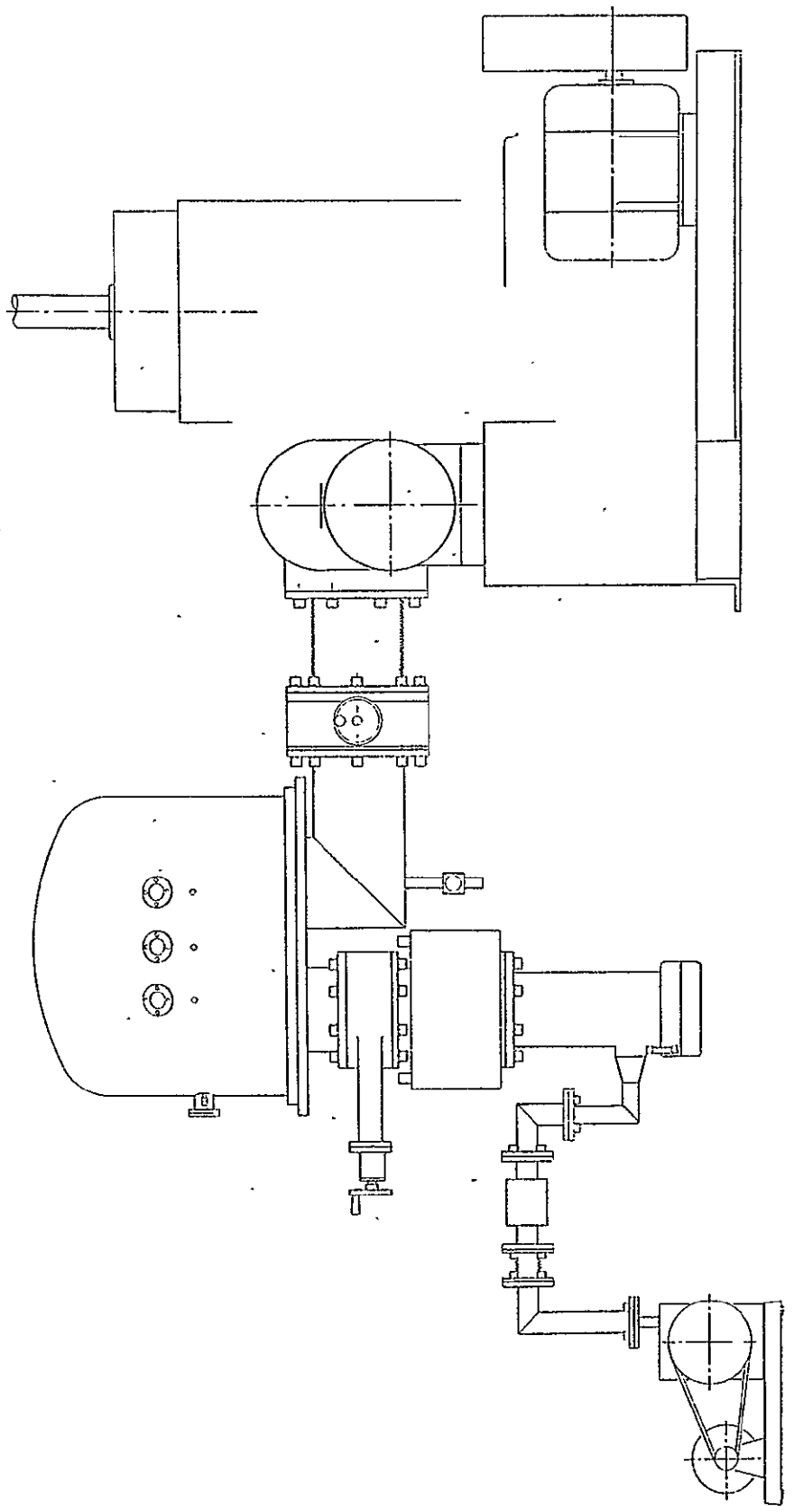

Fig. 6 Overall Layout of High Temperature Emittance Apparatus

cooled leads which enter at the chamber base plate. The flow nozzle is supported from this plate and is adjustable for three positions corresponding to normal, 45° and parallel flow on the specimen. The chamber and base plate are stainless steel with water cooling lines brazed to the chamber walls.

The specimen, electric conductors, is in the form of a strip, 6-in. to 12-in. long and 1/2 in. to 1-in. wide. Width is adjusted for available thickness of material so as not to exceed the voltage and current limitations of the power supply at maximum test temperature. Specimens which are poor or nonelectrical conductors will be heated by two methods. If the material can be applied to a metal substrate or can be formed to accommodate a centrally located element (see Section 7), heating will be done in the same manner as the conductive materials. For materials that cannot be handled in this manner, a platinum strip with a holder at one face will be used to heat the rear surface and edges of the specimen. No calorimetric emittance data can be obtained for this configuration.

Two vacuum systems will be used to provide the range of test pressure. A LN_2 cold trapped, 6-in. diffusion pump will be used for pressures below 10^{-2} mm Hg. A 1200 cfm, two-stage pumping system will provide for pressures from 10^{-1} to atmospheric pressure. Pressure control in this range will be achieved by a bleed valve to introduce air into the line between the chamber and the pumps.

5.3 INSTRUMENTATION

The total and spectral radiometers will use bolometer-type detectors with KBr or Irtran 4 optics. Incident energy will be chopped in order to cover a large range of signal levels through the use of a "lock-in" type amplifier such as that made by Brower Instruments. The near normal viewing unit will include a spectral filter wheel mounted to the detector housing assembly. Detector, optics, and chopper will be assembled into a single unit which is mounted on a flange exterior to the chamber. The flange will include a KBr window and a water-cooled sighting tube within the chamber (Fig. 5) to reduce the possibility of window contamination.

By using rigid mounting to a flange and dowel pins for location of the chamber on the base plate, the necessity of alignment of the radiometer each time a sample is changed is eliminated.

An automatic optical pyrometer, such as manufactured by Pyrometer Instruments Company, will be provided for brightness temperature measurements. Three stations will be provided on the chamber walls for viewing of the specimen surfaces and edge through quartz windows with water-cooled sight tubes.

Chamber pressure in the range of 0.1 to 1000 mm will be measured using an electronic manometer such as the Datametrics, Inc., Baroce l unit. Ionization and thermocouple gauges will be included for pressure measurement in the 10^{-4} to 10^{-1} mm Hg range. The electronic instrument has provision for recorder monitoring of pressure as a function of time.

Feed-throughs for thermocouple and power measuring leads will be provided in the base plate with connections to a reference junction for temperature measurements. The specimen heating power supply will be a controllable saturable core reactor unit for varying power to achieve the desired temperature cycles. A precision current shunt is included in the power lead for measurement of heating current.

Potentiometric instrumentation and automatic data logging equipments will not be provided with the deliverable apparatus as these items are considered to be of the type normally available in a well equipped laboratory facility. During the checkout and calibration period at LMSC, company owned potentiometric and automatic data acquisition equipment currently available in the Thermophysics Laboratory will be used for signal measurement and recording.

A list of all instruments and purchased components, specifying recommended manufactures, and model or part designation, will be supplied in the January 1971 monthly progress report. This information will also be discussed during the January review meeting.

Section 6

INSTRUMENTATION AND MEASUREMENTS

6.1 TEMPERATURE MEASUREMENT

As discussed in Ref. 1, the most difficult problem associated with emittance measurements is that of accurately determining the absolute temperature of the emitting surface. Thermocouples cannot be used with some materials at elevated temperatures because of problems of compatibility of the instrumentation with the test material. At elevated temperatures, large thermal gradients are present through some coated and nonmetallic material so that in-depth temperature measurement cannot be accurately related to surface temperature. Surface temperature thermcouples change the radiant properties of the surface, and it is difficult to relate the temperature of the sensors to the true surface temperature.

Radiation methods are the most useful for measuring surface temperature, but their accuracy is related to the accuracy of the knowledge of the emittance properties of the surface. A number of radiometric methods have been used for temperatures in excess of 400°F. The relationship between measured brightness temperatures and true temperature is a function of the spectral emittance of the surface at the pyrometer mean effective wavelength. In an attempt to eliminate the emittance term from the temperature equation, multiple spectral band pyrometers were developed on the principal that if the material emits as a gray body, i.e., emittance is not dependent upon wavelength, the temperature measurement is independent of emittance. Total radiation pyrometers have also been used, principally at lower temperatures, but again, a value of emittance must be used in the temperature calculation. Figure 7 illustrates the temperature error as a function of assumed emittance for this type of device. Two-temperature pyrometers have also been used with limited success as discussed in Ref. 14 which reviews pyrometry techniques.

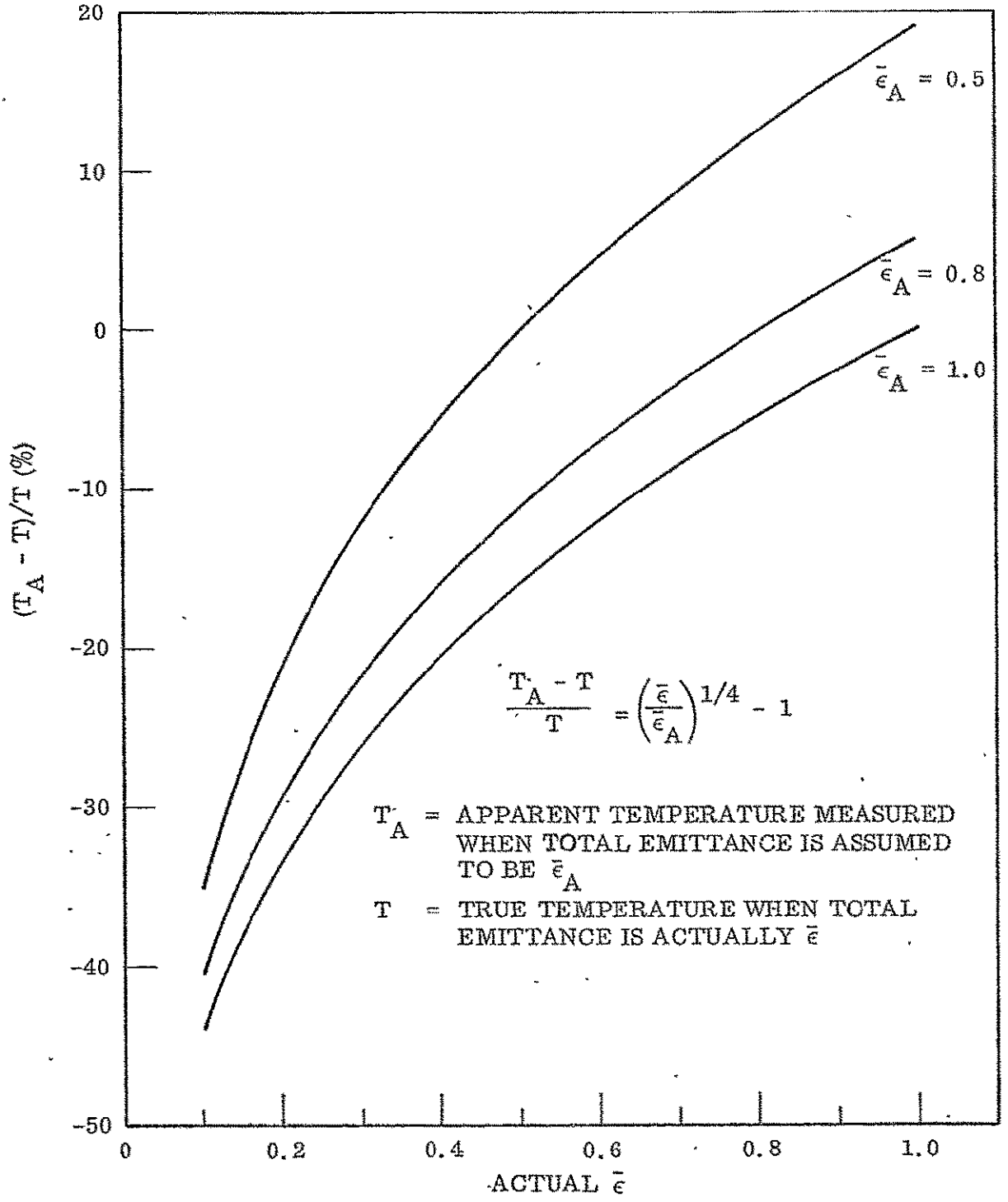

Fig. 7 Temperature Errors Versus Emittance Errors For a Total Radiation Thermopile For Three Assumed Emittance Values

The single-color optical pyrometer appears to be the best choice for this apparatus considering that the specimens will have high values of total emittance (>0.5) and in general will be dark in appearance in the visible region indicating that spectral emittance is high at the shorter wavelengths. Temperature errors for a pyrometer operating at 0.65μ are shown in Figs. 8 and 9 for surfaces having assumed emittance at 0.65μ of 0.5 and 0.8, respectively. To achieve a 1% maximum temperature error at 3140°F, the real emittance of a surface for which ϵ_λ is assumed to be 0.5 must be between 0.45 and 0.55. If the surface emittance (0.65μ) is assumed to be 0.8 and the real spectral emittance is between 0.7 and 0.9, a 1% temperature accuracy will be attained. For materials having a low emittance at 0.65μ, a more accurate knowledge of the two emittances is required to give a small error. For polished metals, the emittance at 0.65μ may be 10 times the total emittance which can result in extremely large temperature errors if spectral data are not available and the 0.65μ value is estimated from a total emittance value.

Two-color pyrometer errors are shown in Fig. 10 for a 0.50 and 0.65μ band instrument. This technique does not improve the temperature measurement accuracy unless bands can be selected at which the emittance values are very nearly equal. Consider a surface which appears dark gray in the visible spectrum, and assume $\epsilon_1 = 0.8$ and $\epsilon_2 = 0.75$. At 3140°F this would introduce a 1% temperature error. However, if ϵ_2 was 0.70, the error would increase to nearly 2.5%.

Clayton (Ref. 13) reports a technique for using an optical pyrometer and a total radiative pyrometer to compute total normal emittance. The emittance accuracy is within 5% if the ratio of $\epsilon_{0.65}$ to ϵ_{TH} is within 0.8 to 1.2. In all cases, some improvement in temperature measurement accuracy can be achieved by obtaining pre- and post-exposure spectral reflectance data at room temperature. The use of this method and the temperature errors for several test materials are discussed further in Section 7.

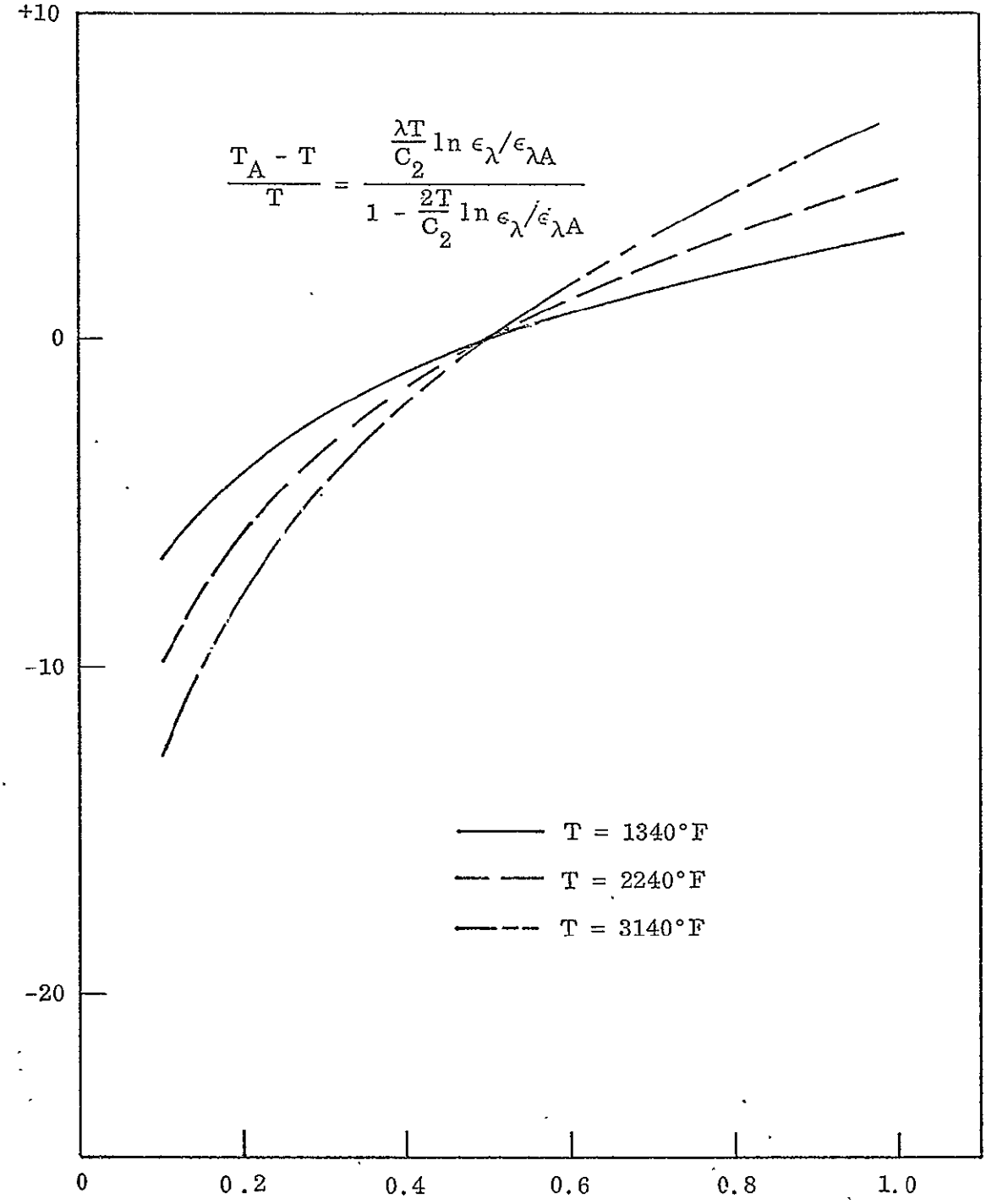

Fig. 8 Temperature Error Versus Emittance Error of an Optical Pyrometer, For Three Temperatures, When the Assumed Spectral Emittance of $\lambda = 0.65\,\mu$ is $\epsilon_{\lambda A} = 0.5$

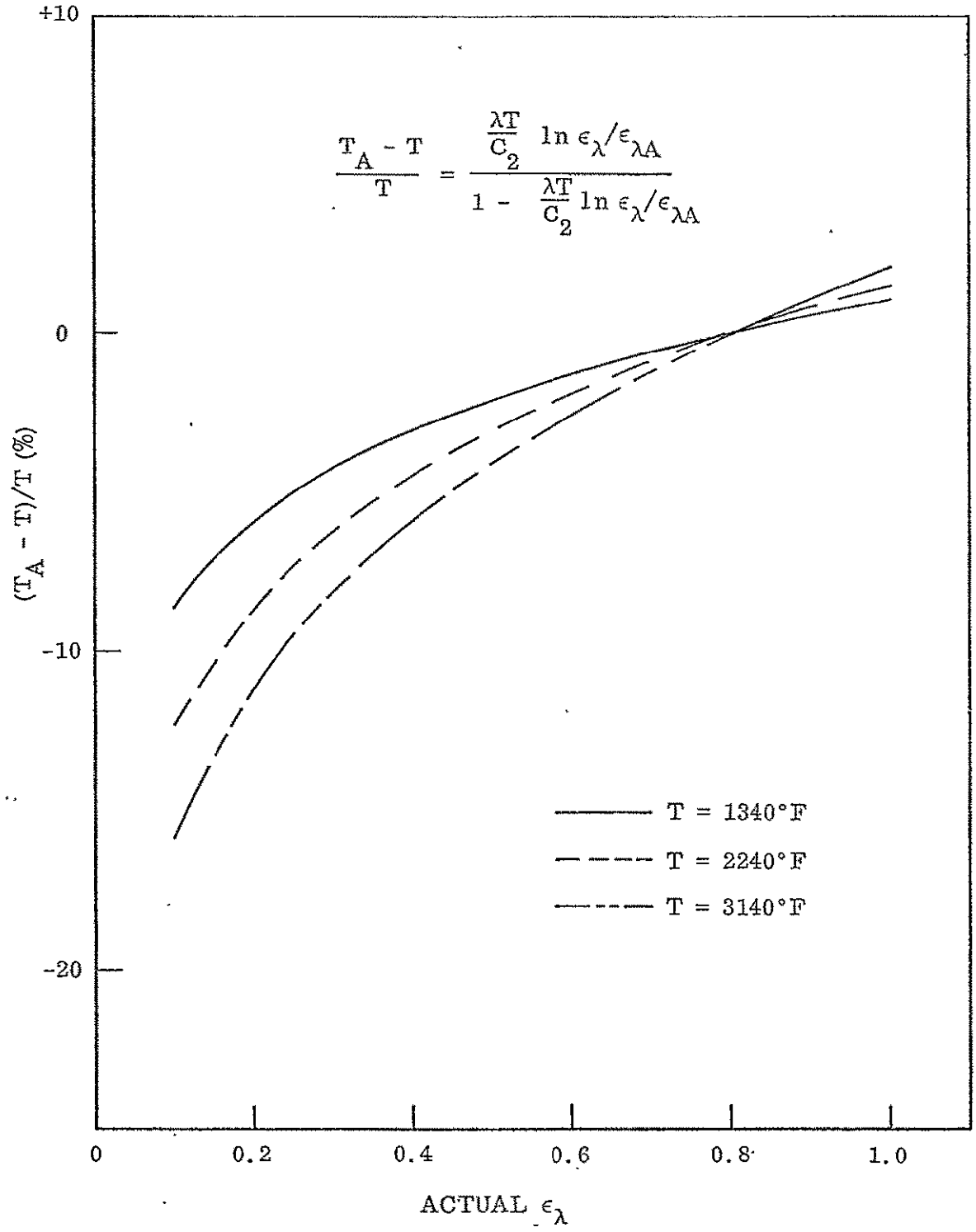

Fig. 9 Temperature Error Versus Emittance Error of an Optical Pyrometer, For Three Temperatures, When the Assumed Spectral Emittance at $\lambda = 0.65\,\mu$ is $\epsilon_{\lambda A} = 0.8$

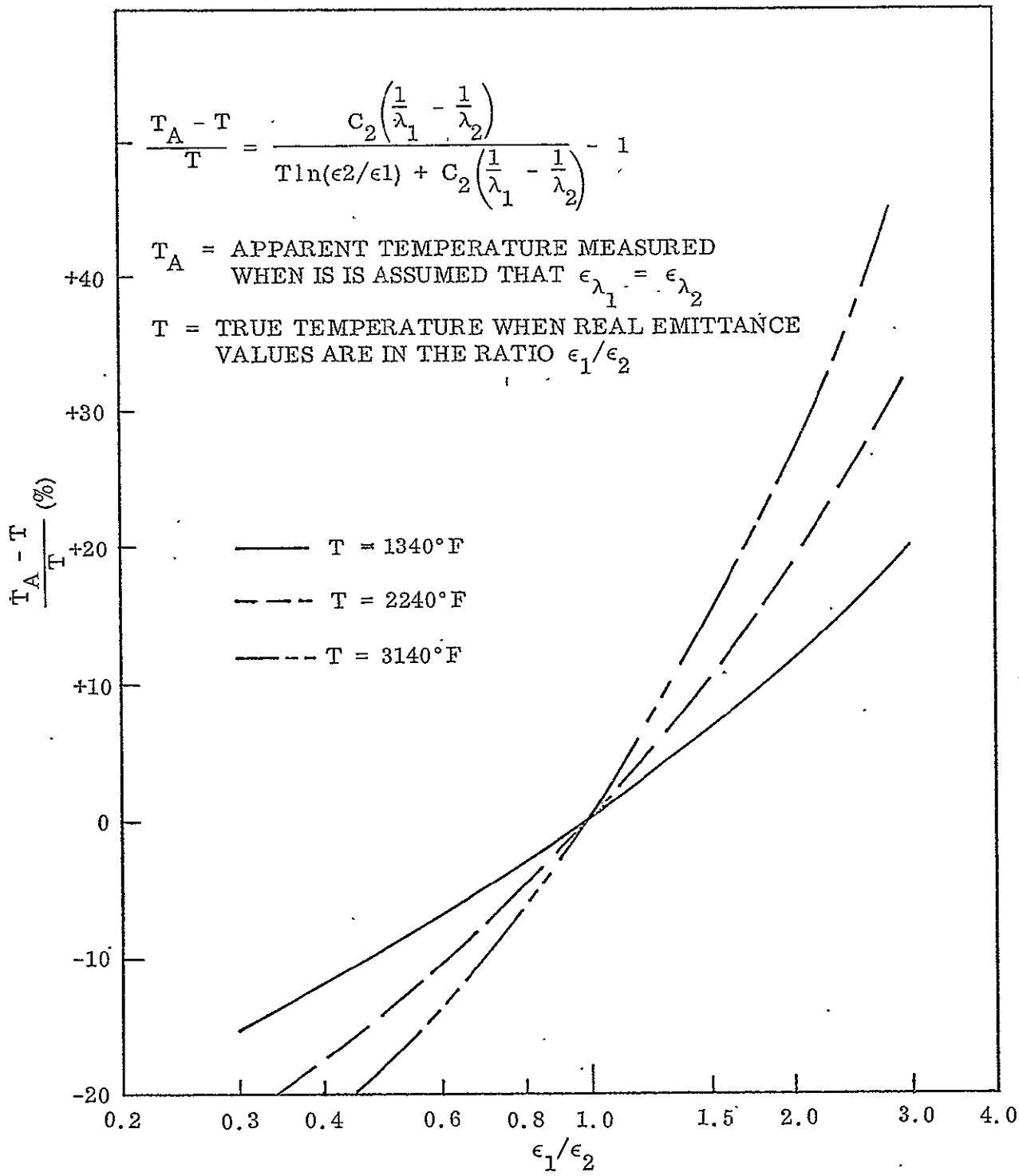

Fig. 10 Temperature Error Versus Error in Graybody Assumption For a Two Color Pyrometer Operating at Wavelengths $\lambda_1 = 0.50\mu$ and $\lambda_2 = 0.65\mu$

6.2 CALORIMETRIC EMITTANCE IN AIR

Total hemispherical emittances for two materials were measured in air as a function of ambient pressure and specimen temperature to evaluate the convective heat losses from the control measuring area for a vertical strip. The data are discussed in detail in Section 7. The vertical strip was selected as no data could be found in the literature for a narrow strip with a very large surface temperature gradient. Convective heat transfer can be computed from literature data for a horizontal orientation of the specimen, short or width dimension either horizontal or vertical. However, for the narrow vertical strip the problem is one of a two-dimensional boundary layer with a very large vertical surface gradient, nearly symmetrical about the center of the strip.

The convective coefficient was computed for the control area by subtracting the radiated power, computed for platinum of known emittance, from the total power (corrected for end conduction losses). Fluid properties were evaluated on the basis of a mean surface to ambient temperature. The data plotted in terms of Nusselt number versus the product of the Grashof and Prandtl numbers is shown in Fig. 11 for three surface temperatures and five ambient pressures. It is interesting to note that the Nusselt number is approximately one order of magnitude greater than would be computed for a wide strip or plate. Some of this discrepancy may be due to the large temperature gradient, but it is felt that a major portion is caused by the two-dimensional boundary layer which for the narrow strip becomes much thinner at the edge.

These data suggest that a horizontal specimen orientation is more desirable for the calorimetric measurement at pressures about 10 mm Hg. If a vertical strip is used, the heat transfer coefficient should be experimentally determined for each size using a material having known radiative properties.

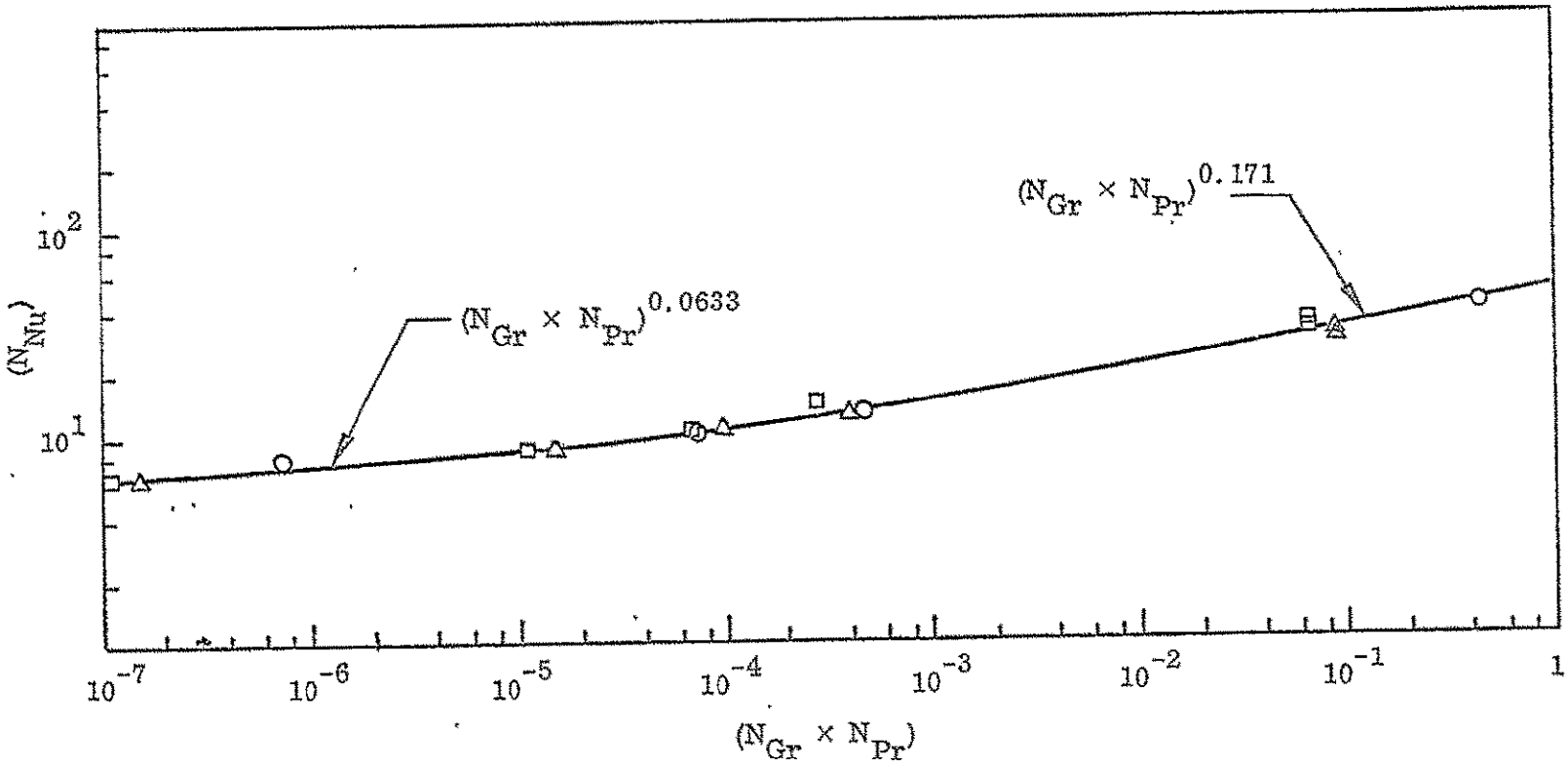

Fig. 11 Experimental Convective Heat Transfer Data From the Vertical Platinum Strip Tests

Section 7

EXPERIMENTAL STUDIES

7.1 INTRODUCTION

Experimental emittance studies of three different materials at elevated temperatures have been made during the past 3-month period in order to evaluate various test and measurement methods used for calorimetric and radiometric determinations of total and spectral emittance. The tests were made using the existing LMSC High Temperature Emittance Apparatus – a heated-strip-type apparatus which has been used extensively in the past for studies of the radiant properties of metals and coated-metal specimens at elevated temperatures in vacuum, e.g., see Refs. 15 and 16. Recent modifications to the apparatus include the addition of a controllable leak in the back-to- air line to the test chamber and a 0- to 50-mm absolute pressure gage in the roughing vacuum line to permit testing in controlled air pressure environments at pressures between 10^{-7} to 50 Torr, and at 760 Torr with the vacuum system off. Otherwise, the total chamber, transfer optics, monochromator and radiation detector systems are essentially the same as described in the aforementioned references.

The three materials examined to date from which the results reported in the remainder of this section were obtained, are: (1) a high temperature, low thermal conductance, ceramic coating material which is currently being developed at LMSC, designated as LI 1500; (2) a preoxidized high temperature, high strength alloy, CL605 – 55% Co, 20% Cr, 15% W, 10% Ni); and (3) a high purity platinum strip. The first two materials were examined because of current interest in their high temperature radiant properties as potentially useful space shuttle materials. Additionally, the ceramic material is one for which accurate surface temperature determinations are difficult to obtain; consequently, its stability and radiant properties at high temperatures are subject to large uncertainties. The platinum sample was selected for

study because of its stable emittance characteristics at elevated temperatures and in oxidizing atmospheres, and therefore as the best material available for an experimental study of gaseous convection and conduction effects on heated-strip specimens in air.

The LI 1500 ceramic coating specimen was tested at several temperatures between 250 and 2350°F in a vacuum (10^{-5} Torr) environment. A tungsten rod was used to heat the specimen; consequently, no tests were attempted in air environments. Radiometric and optical pyrometer measurements were made in order to determine the total and spectral normal emittance characteristics of the specimen but calorimetric determinations of total hemispherical emittance were not obtained. Supplemental information on the radiant properties of this material was obtained from room temperature spectral reflectance measurements with a Cary Model 14 spectrometer (for $0.3\mu \leq \lambda \leq 1.8\mu$) and a Gier-Dunkle heated cavity reflectometer (for $1\mu \leq \lambda \leq 26\mu$), and from spectral reflectance measurements at temperatures up to 2000°F provided by the TRW Systems Group, Redondo Beach, California, using a paraboloid reflectometer (for $0.9\mu \leq \lambda \leq 26\mu$).

The oxidized L605 specimen was tested at temperatures between 250°F and 1600°F in vacuum, at temperatures up to 2000°F in a 1-Torr air environment, and at temperatures up to 1550°F in air (760 Torr). Calorimetric determinations of total hemispherical emittance and radiometric determinations of total and spectral normal emittance were made to evaluate the stability of the oxide coating and to indicate the effects of convective heat losses on the emittance determinations.

The platinum specimen has been tested at temperatures between 750 and 2000°F in air pressure environments of 10^{-5}, 1, 10, 25, 50, and 760 Torr, and up to 2500°F in vacuum. Total hemispherical, total normal, and spectral normal emittance values are reported and the effects of convection at each pressure on the steady-state heat balance term for the specimen are indicated.

Additional tests of the platinum sample at 2500°F in the various air pressure environments will be completed in the near future, and similar tests are planned for a coated refractory metal specimen (Cb 752 alloy). The results of these studies will be analyzed to indicate the test and measurement limitations of the present apparatus and for ideas concerning possible improvements in specimen design and test instrumentation that could be incorporated into a new test apparatus design. Results of the tests completed to date are discussed in the following subsections for each material.

7.2 LI 1500 CERAMIC COATING STUDY

7.2.1 Sample Description

This sample came in the form of a coated ceramic (silica base) tube with an overall o.d. of 0.480 in. and an i.d. of 0.135 in. The thickness of the coating was 0.030 in. and was uniform to within 0.001 in. along the length of the tube. The coating material is an oxide-dopped slip-cast silica, dark green in color. The tube was cut into five sections (two 2.5-in. long end sections, two 0.5-in. long inner sections, and one 1.0-in. long center test section) which were slipped over an 8-in. long, 0.125-in. diameter tungsten heater rod as shown in Fig. 12. An alumina bead was used to support the tube sections above the lower, water-cooled, electrode clamp at a height which centered the 1-in. long test section at the mid-length of the heater rod and on the optical axes of the viewing windows for the detectors and the optical pyrometer.

Four thermocouples were attached to the center test section of the sample to obtain surface temperature measurements, and to indicate the radial temperature gradients from the heater rod to the surface. After placing the thermocouples at the locations shown in Fig. 12, they were held in place by cementing the 3-mil lead wires to the surface with more of the coating material which was available in a fast-setting liquid form. This method was satisfactory for holding the thermocouples in place but was a poor choice from the standpoint of obtaining accurate surface temperature measurements. The uneven overcoat of cement material covering the thermcouple junctions

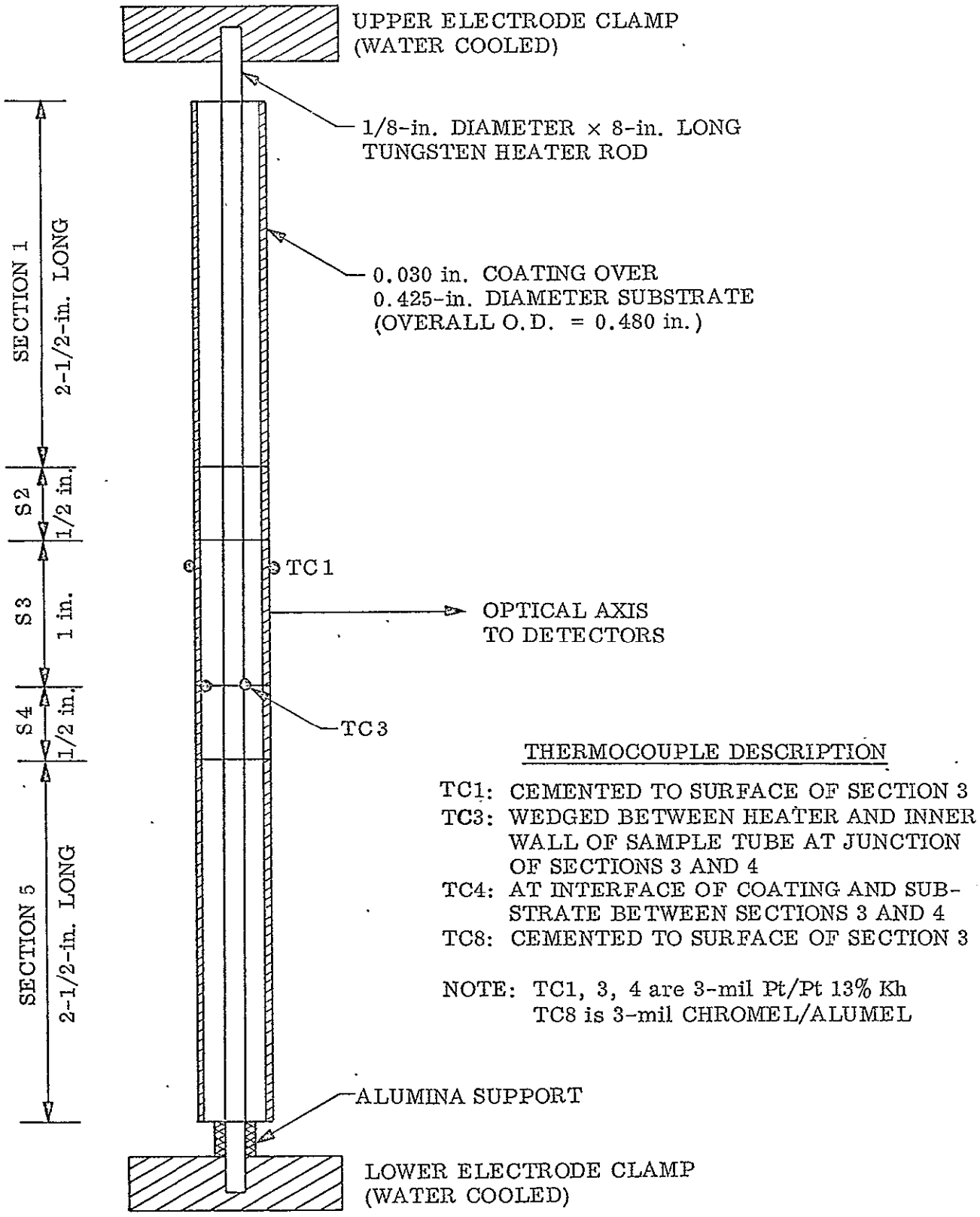

Fig. 12 LI 1500 Ceramic Coating Test Specimen

was from 15- to 25-mils thick and these variations in thickness resulted in large variations in temperature at the surface of the sample and low temperature readings from the thermocouples. Estimates of the thermocouple temperature errors are tabulated and discussed in the next subsection.

7.2.2 Temperature Measurements

Three methods were investigated for determining surface temperatures of the LI 1500 test specimen during this study. The methods were (1) surface thermocouple measurements; (2) optical pyrometer temperature measurements for a small, blackbody cavity machined in the specimen; and (3) optical pyrometer measurements of the surface brightness temperature. Only the latter method proved to give reasonably accurate indications of the true surface temperature.

Pyrometer temperature measurements on a small (0.020-in diameter by 0.060-in deep) cavity drilled into the surface of the specimen were obtained during a preliminary test which was made to determine if the sample could be heated sufficiently for observations with a pyrometer, i.e., to $T_s \geq 1400°F$. This test was made prior to attachment of the thermocouples, and the surface brightness temperature of the specimen at $T \approx 1500°F$ was observed to be uniform to within $\pm 10°F$ at that time. Brightness temperature readings from the reference cavity were observed to be unreasonably high and the cause was attributed to the large radial temperature gradient through the specimen. The use of this method was therefore abandoned and the sample thermocouples were attached, as described earlier.

The intended purpose of the thermocouples was to provide temperature measurements in the region $250°F \leq T < 1400°F$ where pyrometer measurements were not possible. Subsequent measurements of emittance of these lower temperatures resulted in total normal emittance values which appeared to be high by as much as 25 to 30%, indicating that the surface thermocouple temperatures were on the order of 6 to 8%. At test temperatures above 1400°F, where the thermocouple temperatures could be compared with the pyrometer temperature readings, the thermocouple error appeared to be of the same magnitude. These comparisons at several temperatures between 1400°F and 2350°F are shown in Table 4.

Table 4

COMPARISON OF THERMOCOUPLE AND OPTICAL PYROMETER DETERMINATIONS OF SURFACE TEMPERATURES FOR THE LI1500 SPECIMEN

Test Number and Temperature Cycle	Surface Temperature		Apparent Thermocouple Error (%)
	Thermocouple Measurements (°F)	Pyrometer Measurements[a] (°F)	
T4 /1	1290	1429	- 7.4
T8 /2	1283	1402	- 6.4
T9 /2	1524	1641	- 5.6
T10/2	1767	1884	- 5.0
T11/2	2095	2354	- 9.2
T15/3	1569	1800	-10.2
T16/3	1909	2192	-10.7

(a) ϵ_λ for the surface at $\lambda = 0.65\mu$ assumed to be 0.80.

At the 2350°F, temperature level, the temperature indication from the Pt/Pt 13% Rh thermocouple was observed to drop about 80°F, relative to the chromel/alumel thermocouple reading. The reason for this change was not ascertained but is presumably due to a reaction between the platinum and the hot, silica-base ceramic. (See Ref. 17.) Similar losses in thermoelectric output were observed for the other two platinum thermocouples, and at the highest test temperature, TC 3-adjacent to the tungsten heater rod, open-circuited. The last three thermocouple measurements shown in Table 4 are from the chromel/alumel thermocouple and the increase in apparent thermocouple error, relative to the pyrometer measurements, indicates that these alloys also deteriorated and that the damage was permanent.

7.2.3 Emittance Determinations

Table 5 summarizes the total normal emittance values that were determined for this material using several different methods. The values listed under Method 1 were

Table 5

TOTAL NORMAL EMITTANCE VALUES FOR LI1500 CERAMIC COATING BY SEVERAL METHODS

Temperature (°F)	Total Normal Emittance				
	Method 1	Method 2	Method 3	Method 4	Method 5
80	0.85				
250	0.84	0.89	1.01		
500	0.82	0.84	0.99		
750	0.77	0.80	0.90		
1000	0.70	0.76	0.88		
1250	0.65	0.73	0.82		
1500	0.60	0.70	0.77	0.61	0.58
1750	0.55	0.68	0.73	0.56	0.51
2000	0.51	0.67	0.70	0.53	0.47
2350	0.47			0.49	0.41
2500	0.46				

Method 1: Integration of spectral reflectance measurements at room temperature.

Method 2: Integration of spectral reflectance measurements at temperatures between 200°F and 2000°F. Note: This specimen was previously exposed to radiant heating tests and had a lower reflectance in the $0.30\mu \leq \lambda \leq 1.8\mu$ spectral region than the specimen measured for Method 1.

Method 3: Direct radiometric measurements using temperatures indicated by surface thermocouples.

Method 4: Same as Method 3 but using temperatures indicated by optical pyrometer measurements of T_b and assuming $E_\lambda\ (\lambda = 0.65\mu) = 0.80$.

Method 5: Boeing's Two-Color radiometric method assuming $\epsilon_\lambda\ (\lambda = 0.65\mu) = \epsilon_{TN}$.

computed from room temperature spectral reflectance measurements from a 1-in. diameter disk specimen of the same coating material and of approximately the same thickness. The accuracy of emittance values obtained by this method becomes increasingly uncertain for higher temperature because the changes in spectral reflectance with temperature are not accounted for. A plot of the room temperature spectral emittance characteristics for the LI1500 coating materials is shown in Fig. 13, where it is assumed that the material is opaque at all wavelengths, ($\tau_\lambda = 0$), and that $E_\lambda = 1 - R_\lambda$. The reason for the apparent decrease in total normal emittance with increasing temperature is seen due to the presence of the broad, low-emittance (high reflectance) band between $\lambda = 0.7\mu$ and $\lambda = 4.0\mu$.

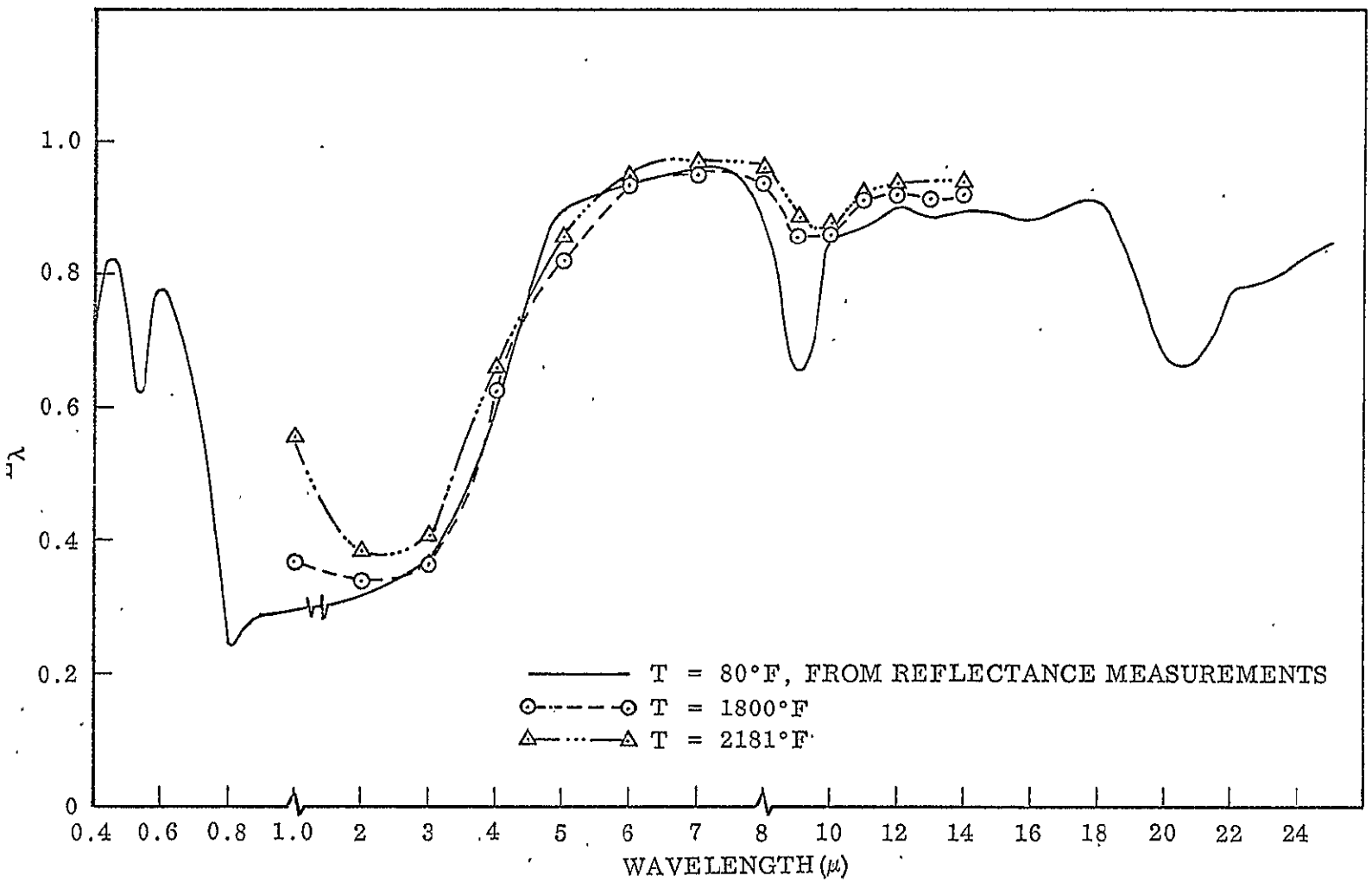

Fig. 13 Spectral Emittance of LI 1500 Ceramic Coating

The values listed under Method 2 of the table were computed in the same manner as for Method 1, but the spectral reflectance measurements in this case were obtained from a heated specimen at temperatures of 200, 1000, 1500, and 2000°F. These measurements were made for LMSC by the Thermophysics Section Laboratory of TRW Systems, Redondo Beach, California, using a paraboloid reflectometer (Ref. 18). High temperature total normal emittance values computed from measurements like these are more reliable than those from room temperature measurements because the changes in spectral emittance with temperature are accounted for. These total normal emittance values also appear to drop with increasing temperature, but not nearly as much as indicated by the values under Method 1. Not all of the difference can be attributed to differences in the measurement methods, however, because the sample investigated at TRW was from a different batch of material and had been previously exposed to a radiant heating test which resulted in its having a significantly higher room temperature reflectance in the region $0.35\mu \leq \lambda \leq 1.8\mu$.

The values listed under Method 3 in the table are those that were obtained from the heated tube specimen with the assumption that the temperature of the specimen was that indicated by the surface thermocouples. These values are initially high by about 25% at the low temperatures and end up about 40% high, relative to the Method 1 values, at 2000°F. As discussed earlier, these errors are consistent with the apparent temperature errors for the surface thermocouples on this specimen.

The values listed under Method 4 correspond to those under Method 3 but using the temperatures indicated by the optical pyrometer readings of surface brightness temperatures. These values tend to support the validity of those obtained by Method 1, and are also in good agreement with the spectral emittance determinations made at 1800°F and 2180°F which are shown in Fig. 13. This agreement between the spectral and total emittance values obtained by Methods 1 and 4 strengthens the belief that the reason for the higher emittance values by Method 2 was due to real sample-composition differences rather than to differences in the measurement methods.

The emittance values listed under Method 5 were obtained using the Boeing Graybody method, where the total radiation detector signal is converted to an equivalent blackbody temperature and the optical pyrometer brightness temperature measurement is converted to a true surface temperature. These values appear to be consistent with the predicted errors for this method when the sample is nongray, e.g., the error in the value at 1500°F (0.58) appears to be small, where ϵ_λ is still close to ϵ_{TN}, but is much larger at t = 2350°F, due to the further drop in ϵ_{TN} relative to ϵ_λ.

Section 8
FUTURE ACTIVITY

The activities during the next monthly reporting period will be devoted to facilities design studies with particular emphasis on radiometric instrumentation, flow nozzle, and the specimen mounting and tension control arrangement.

Section 9

REFERENCES

1. Development of Techniques and Associated Instrumentation for High Temperature Emissivity Measurements, First Quarterly Progress Report, Contract NAS 8-26304 No. N-JF-70-1, Oct 1970

2. C. T. Edquist and M. G. Strapp, A Sphere-Cone Heating Analysis Program, ENVY LMSC Report TIAD 837, 13 Oct 1966

3. K. T. Edquist, Boundary Layer Thickness Calculations, LMSC Report TIAD 790, 21 Jun 1965

4. E. Reshotleo and I. E. Beckwith, Compressible Laminar Boundary Layer Over a Yawed Infinite Cylinder With Heat Transfer and Arbitrary Prandtl Number, NACA TN 3986, Jun 1957

5. I. E. Beckwith and J. J. Gallager, Local Heat Transfer and Recovery Temperature on a Yawed Cylinder at a Mach Number of 4.15 and High Reynolds Number, NASA TR R-104, 1961

6. R. A. Perkins and C. M. Packer, Coatings for Refractory Metals in Aerospace Environments, AFML-TR-65-351, Sep 1965

7. N. G. Kulgein, "Heat Transfer From a Nonequilibrium Turbulent Boundary Layer to Catalytic Surfaces," AIAA J., Vol. 3, Feb 1965

8. L. Kaufman and H. Nesor, Stability Characterization of Refractory Materials Under High Velocity Atmospheric Flight Conditions, AFML-TR-69-84, Part I, Vol. I, Mar 1970

9. L. Kaufman and H. Nesor, Stability Characterization of Refractory Materials Under High Velocity Atmospheric Flight Conditions, AFML-TR-69-84, Part III, Vol. III, Feb 1970

10. H. Goldstein, Private communication, Nov 1971

11. W. A. Clayton and J. M. Gunderson, Calibration of Mass Transport Capability of Re-Entry Materials Evaluation Facility X-33, Doeing Report DS-SR-214 MP, 13 Dec 1963

12. J. D. Buckley and B. A. Stein, Preliminary Investigation of the Dynamic Oxidation of JT Graphite Composites at Surface Temperatures Between 4000°F and 5000°F, AFML-TR-66-174, P595, Jul 1966

13. W. K. Stratton, et al., Advance in Materials Technology Resulting From the X-20 Program, AFML-TR-64-396, Mar 1965

14. A. G. Enslie and H. H. Blau, Jr., "On the Measurement of Temperatures of Unenclosed Objects by Radiation Methods," J. Electrochem. Soc., Oct 1959, p. 877

15. R. E. Rolling, A. I. Funai, and J. R. Grammer, Investigation of the Effect of Surface Condition on the Radiation Properties of Metals, AFML-TR-64-363, Parts I and II

16. G. R. Cunnington, A. J. Funai, J. R. Grammer, and R. F. Karlak, Program ASTEC, Part II, Jun 1966

17. E. D. Zysk, "Platinum Metal Thermocouples," Temperature – Its Measurement and Control in Science and Industry, Vol. 3, Part 2, Reinhold Publishing Corp., New York, 1962

18. B. E. Newman, "Emittance of Ablative Materials," prepared by TRW Systems for NASA under Contract NAS 9-4518

Appendix A
BOUNDARY LAYER FLOW PROPERTIES

Temperature, density, and equilibrium are species concentration profile for five altitudes and three vehicle locations are presented in Figs. A-1 through A-17. Computation procedures are discussed in Section 3 of this report.

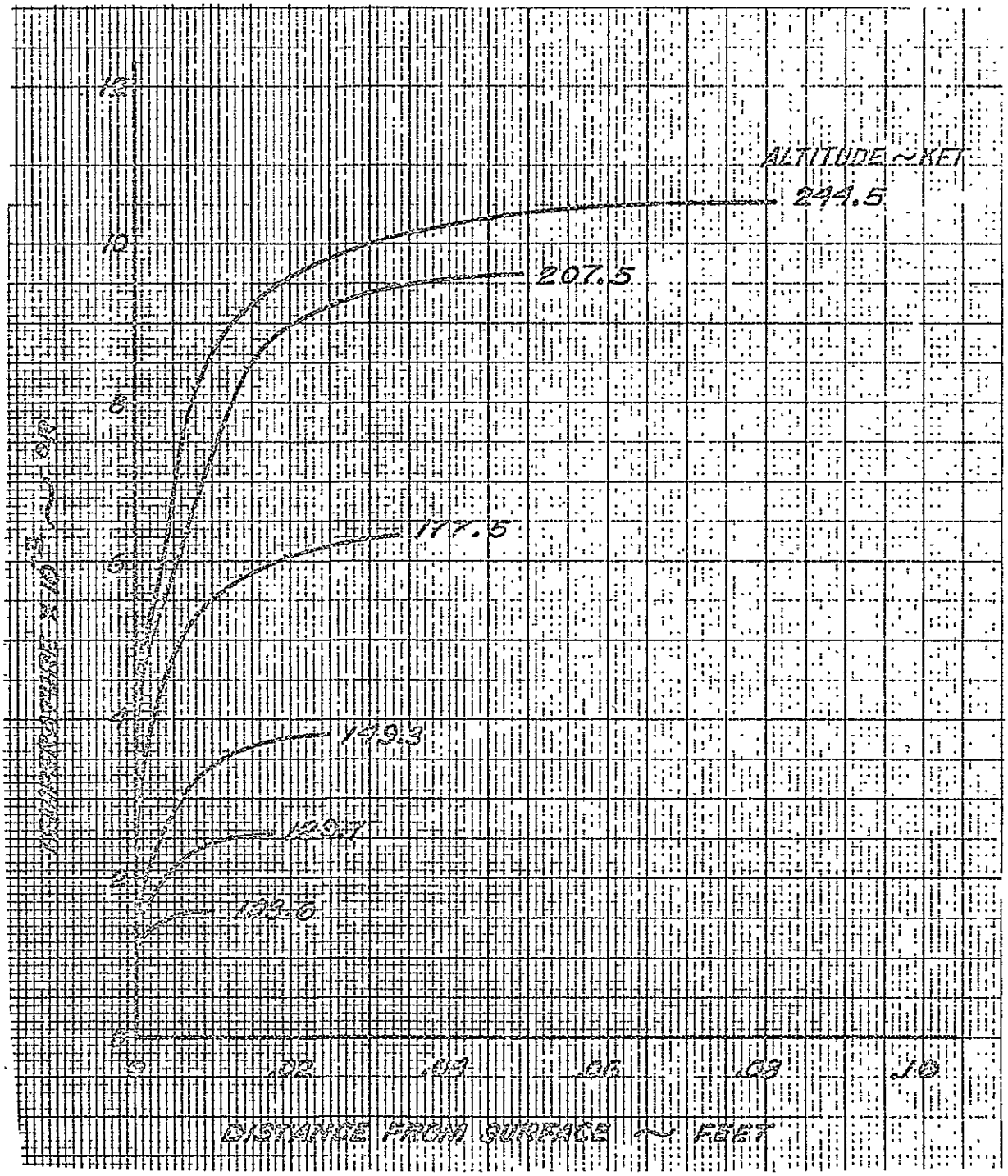

Fig. A-1 Boundary Layer Temperature Profile at Stagnation Point

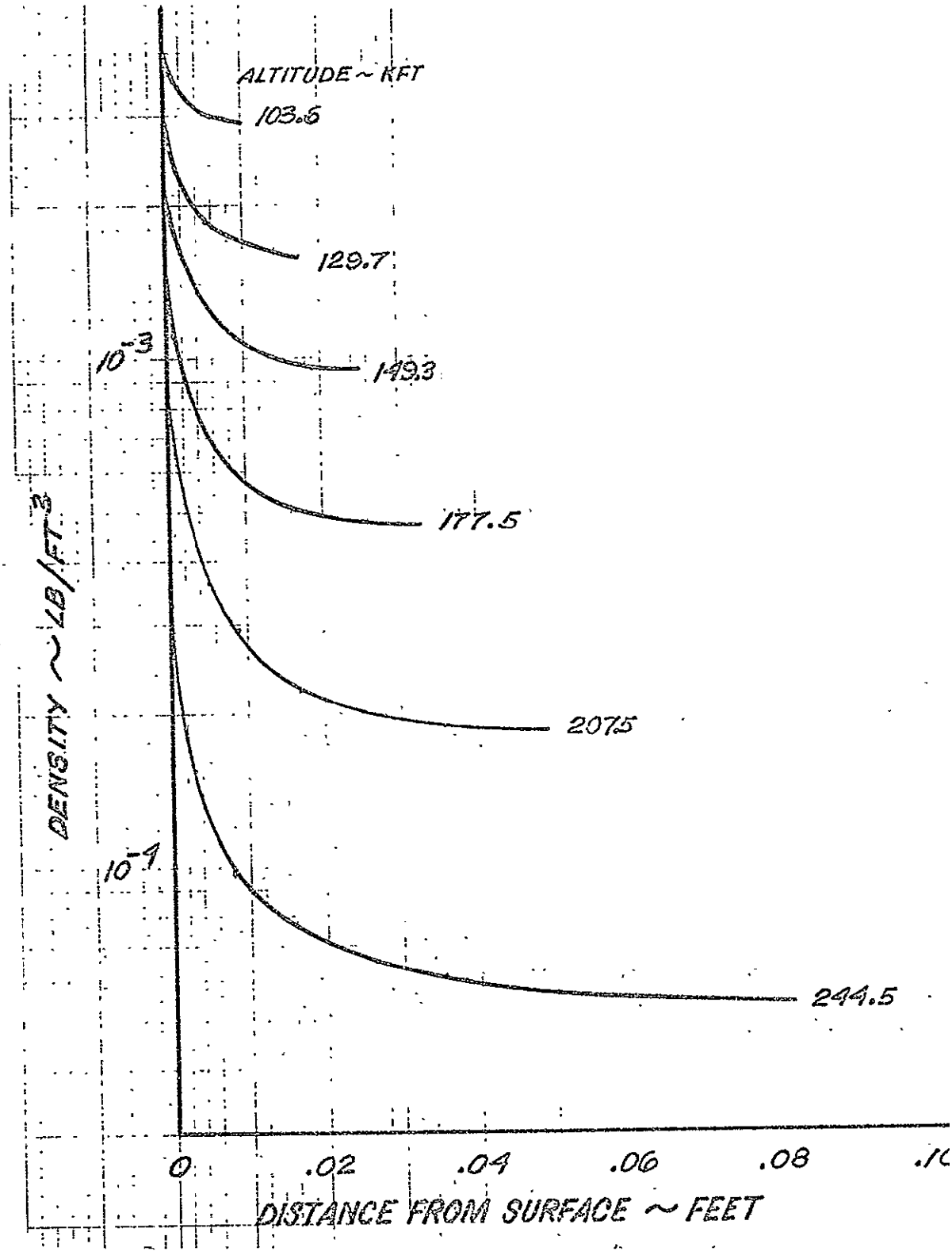

Fig. A-2 Boundary Layer Density Profile at Stagnation Point

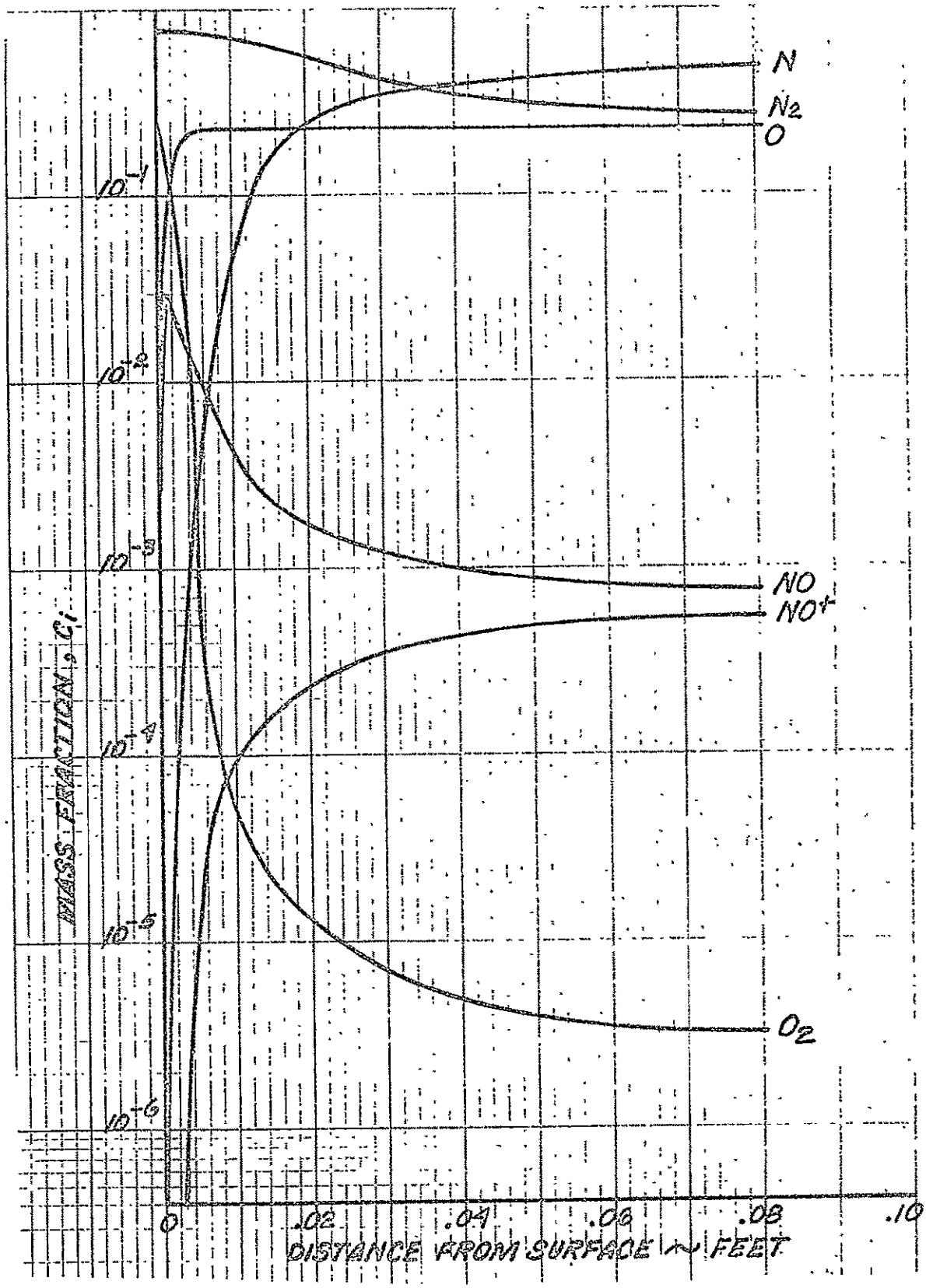

Fig. A-3 Equilibrium Air Species Concentration Profile at Stagnation Point for 244.5 kft Altitude

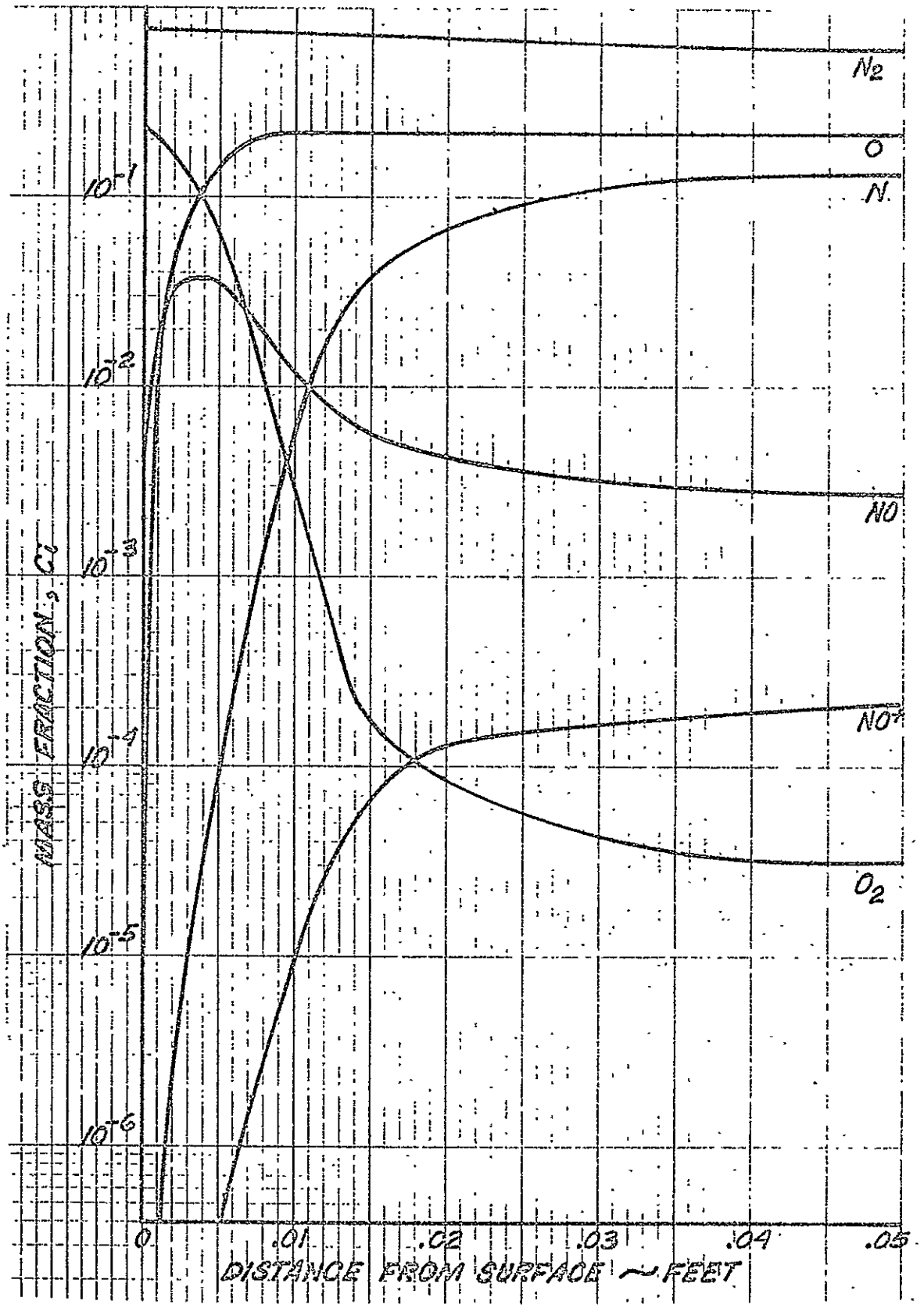

Fig. A-4 Equilibrium Air Species Concentration Profile at Stagnation Point for 207.5 kft Altitude

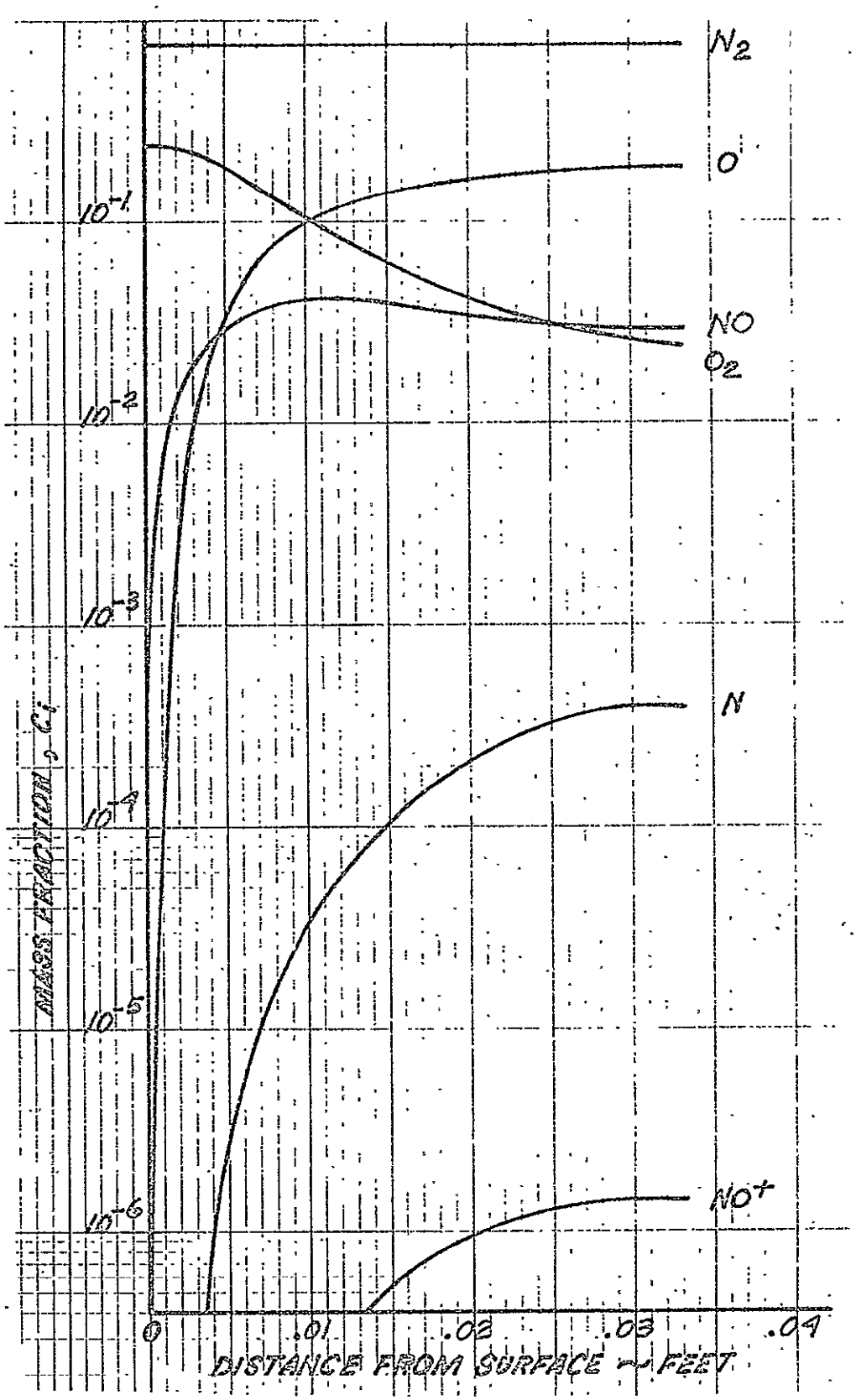

Fig. A-5 Equilibrium Air Species Concentration Profile at Stagnation Point for 177.5 kft Altitude

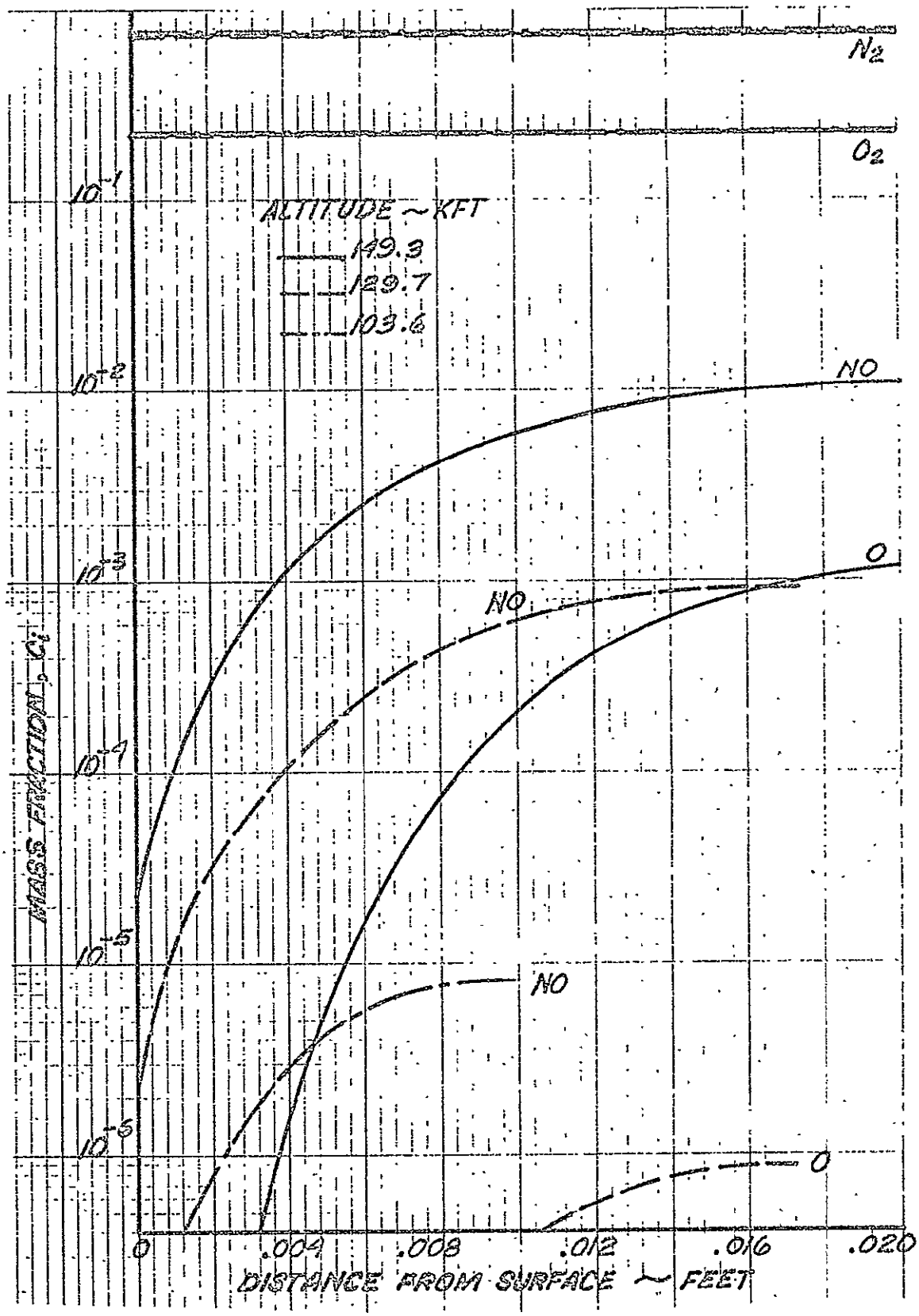

Fig. A-6 Equilibrium Air Species Concentration Profile at Stagnation Point for Three Altitudes

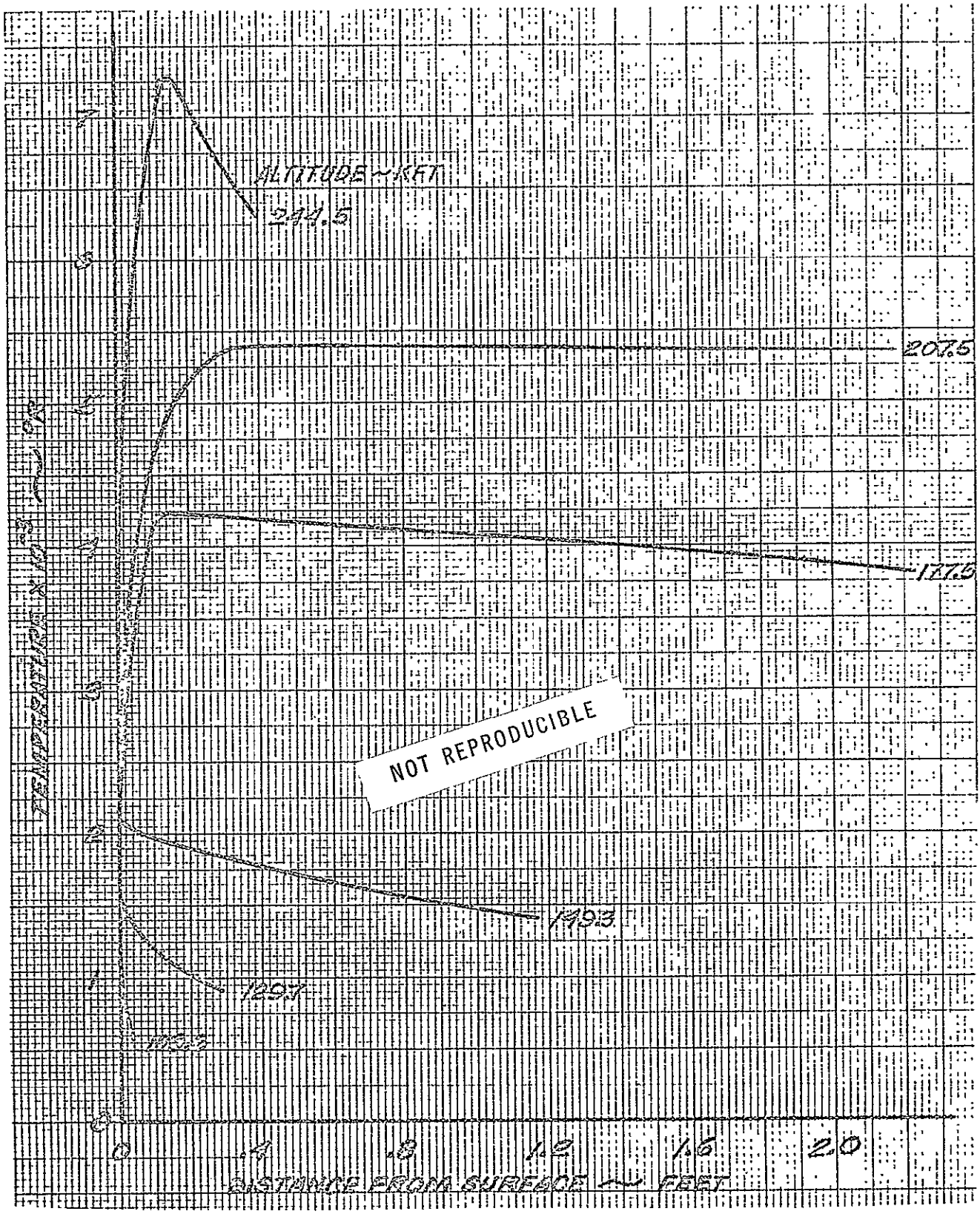

Fig. A-7 Boundary Layer Temperature Profile at X/L = 0.5 on Lower Surface

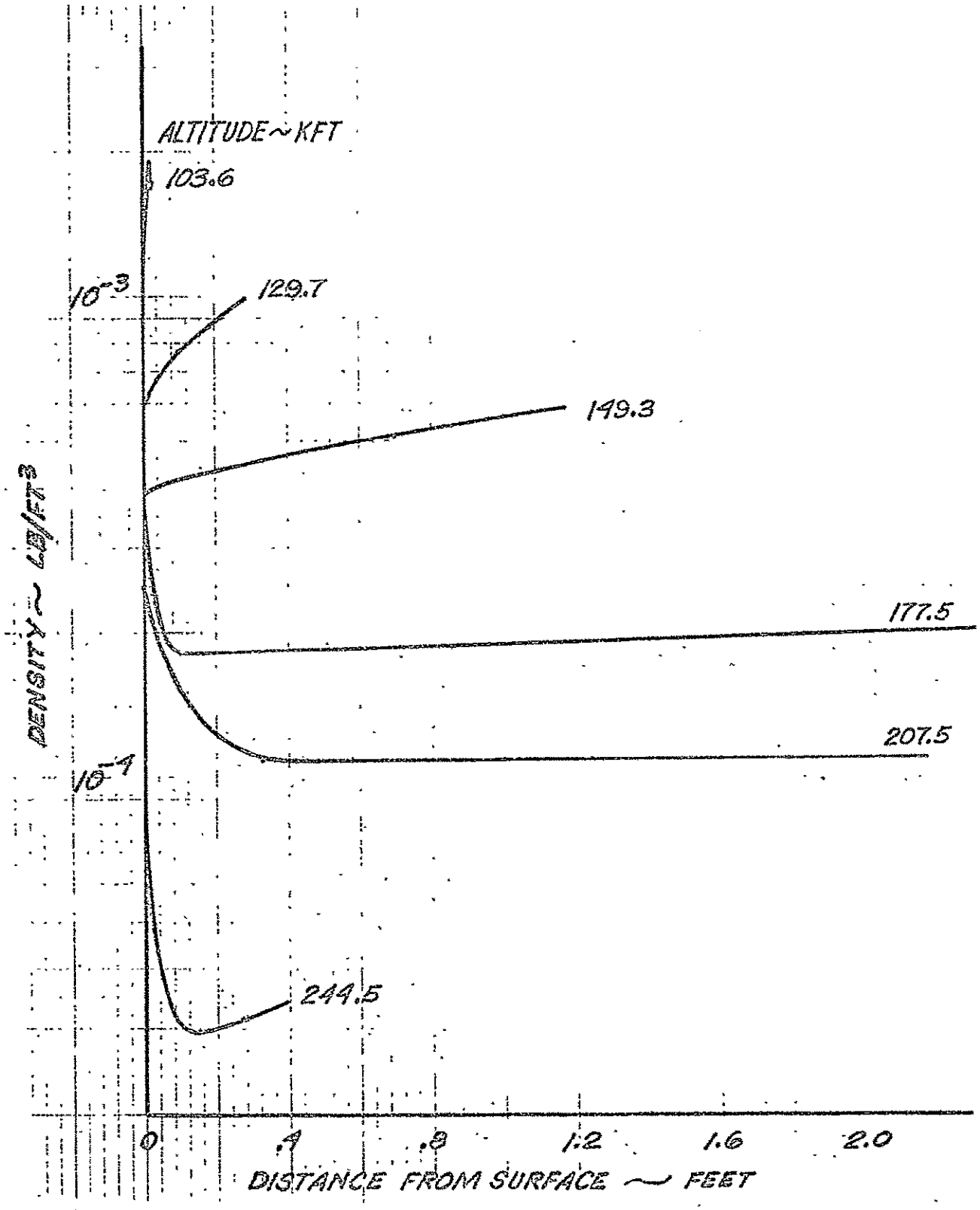

Fig. A-8 Boundary Layer Density Profile at X/L = 0.5 on Lower Surface

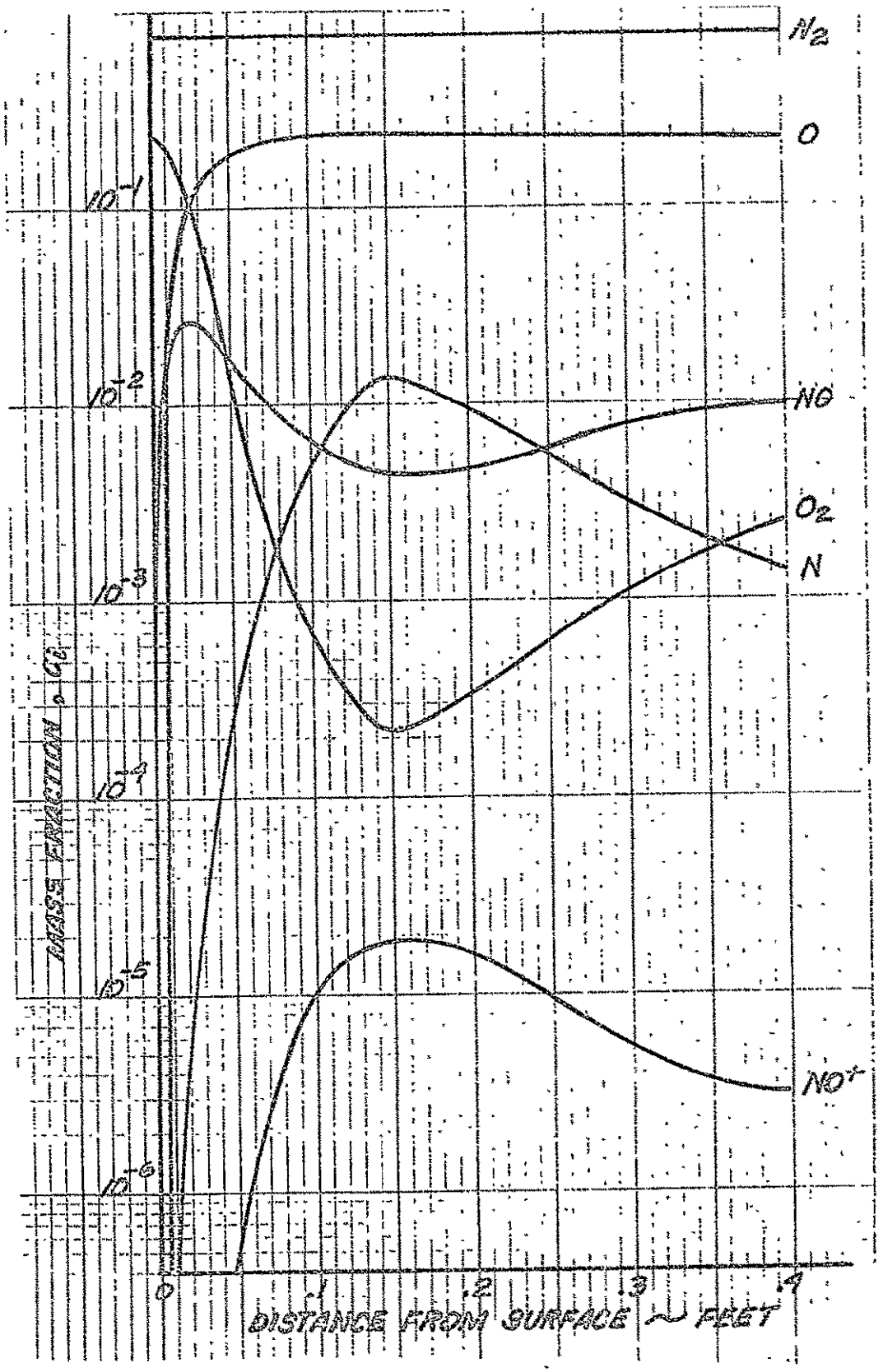

Fig. A-9 Equilibrium Air Species Concentration Profile at X/L = 0.5 on Lower Surface for 244.5 kft Altitude

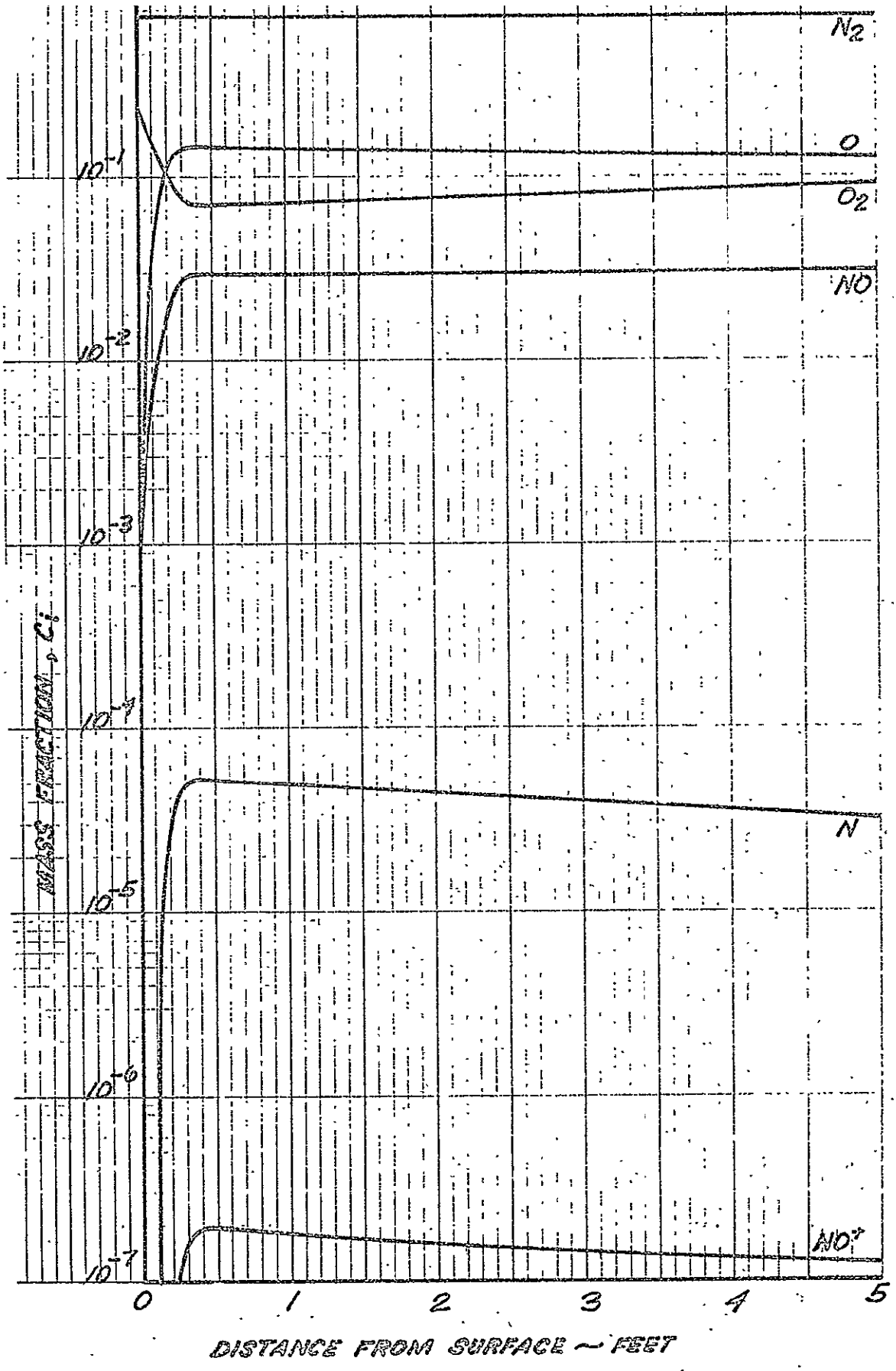

Fig. A-10 Equilibrium Air Species Concentration Profile at X/L = 0.5 on Lower Surface for 207.5 kft Altitude

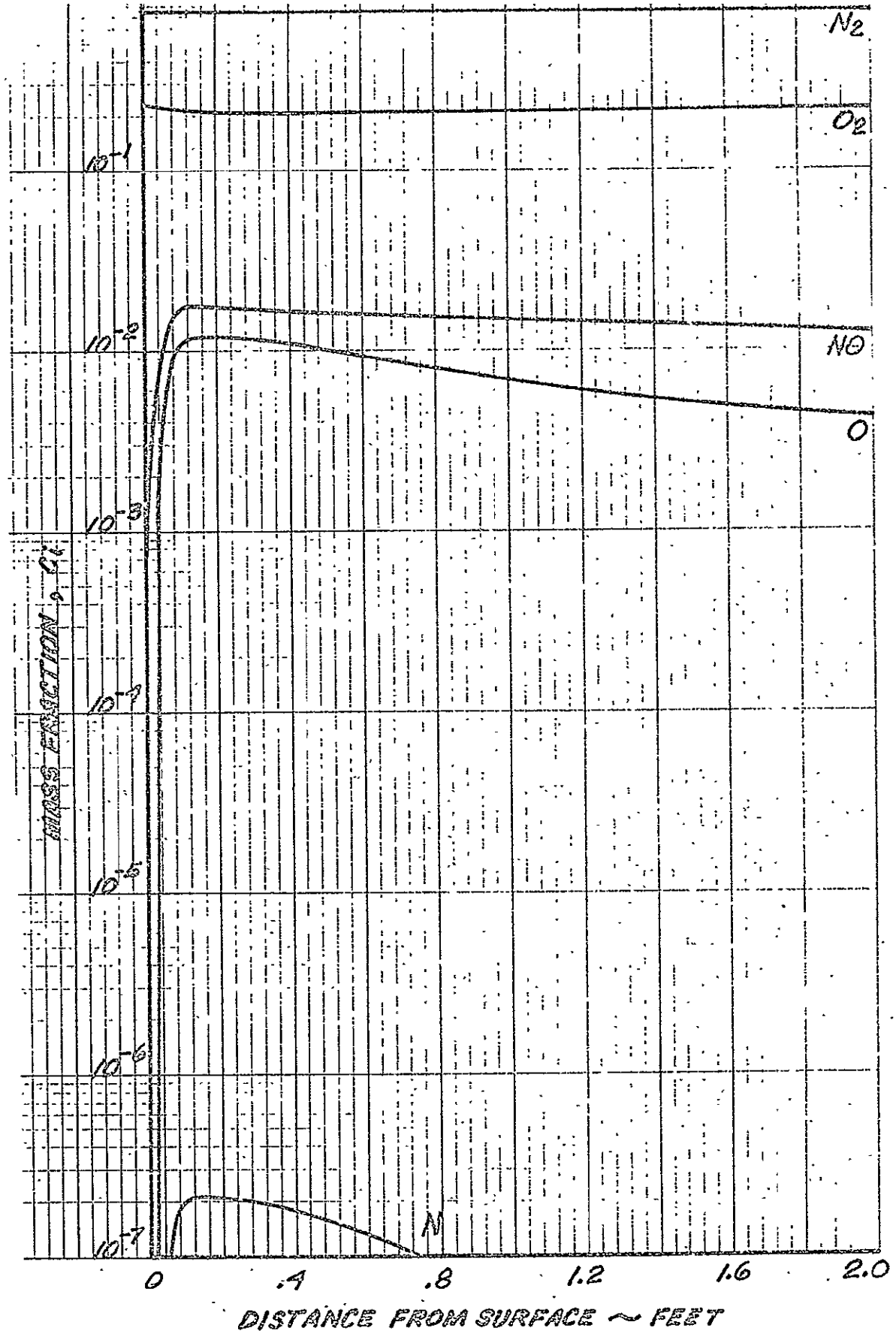

Fig. A-11 Equilibrium Air Species Concentration Profile at X/L = 0.5 on Lower Surface for 177.5 kft Altitude

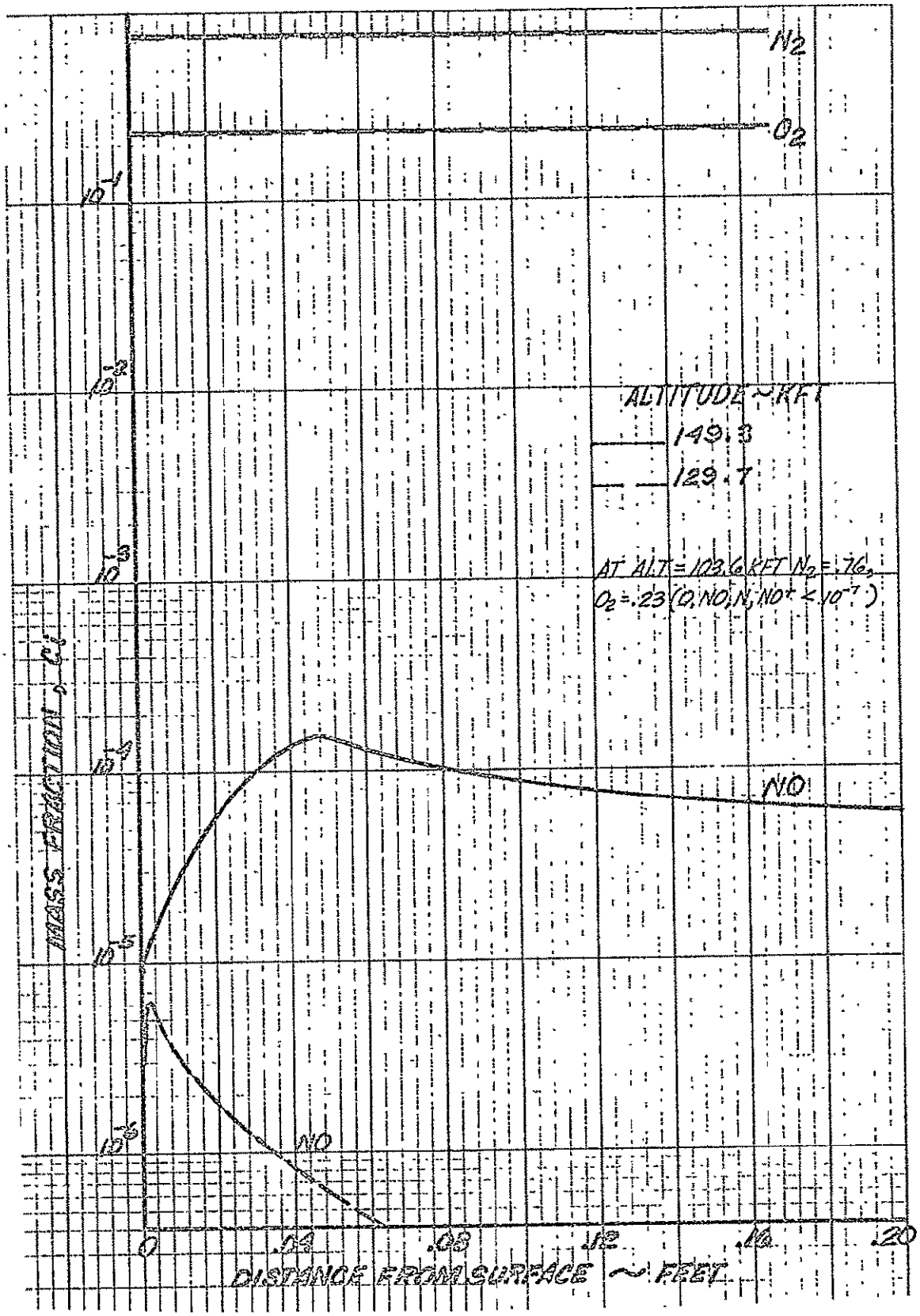

Fig. A-12 Equilibrium Air Species Concentration Profile at X/L = 0.5 on Lower Surface for Two Altitudes

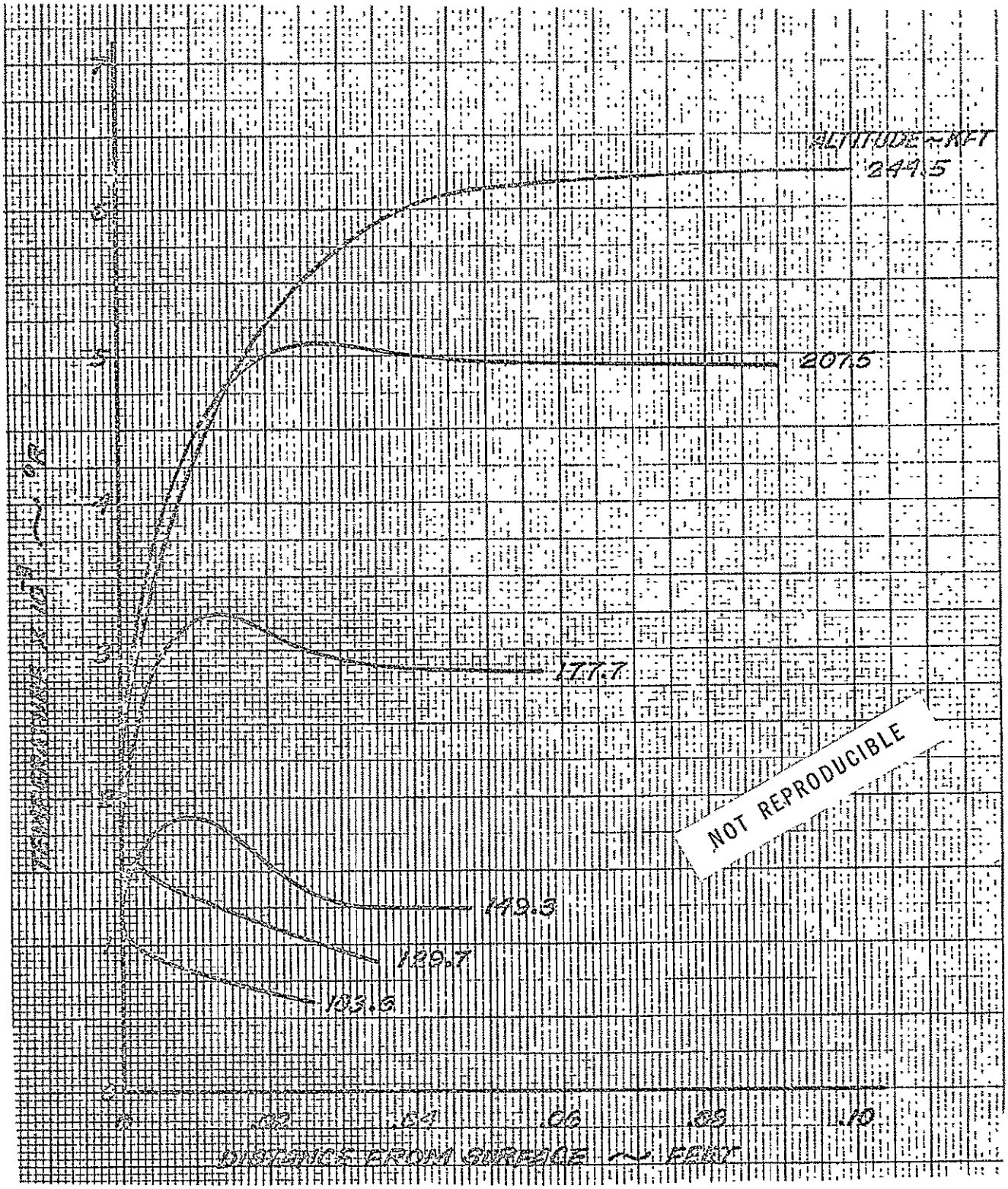

Fig. A-13 Boundary Layer Temperature Profile Along Leading Edge

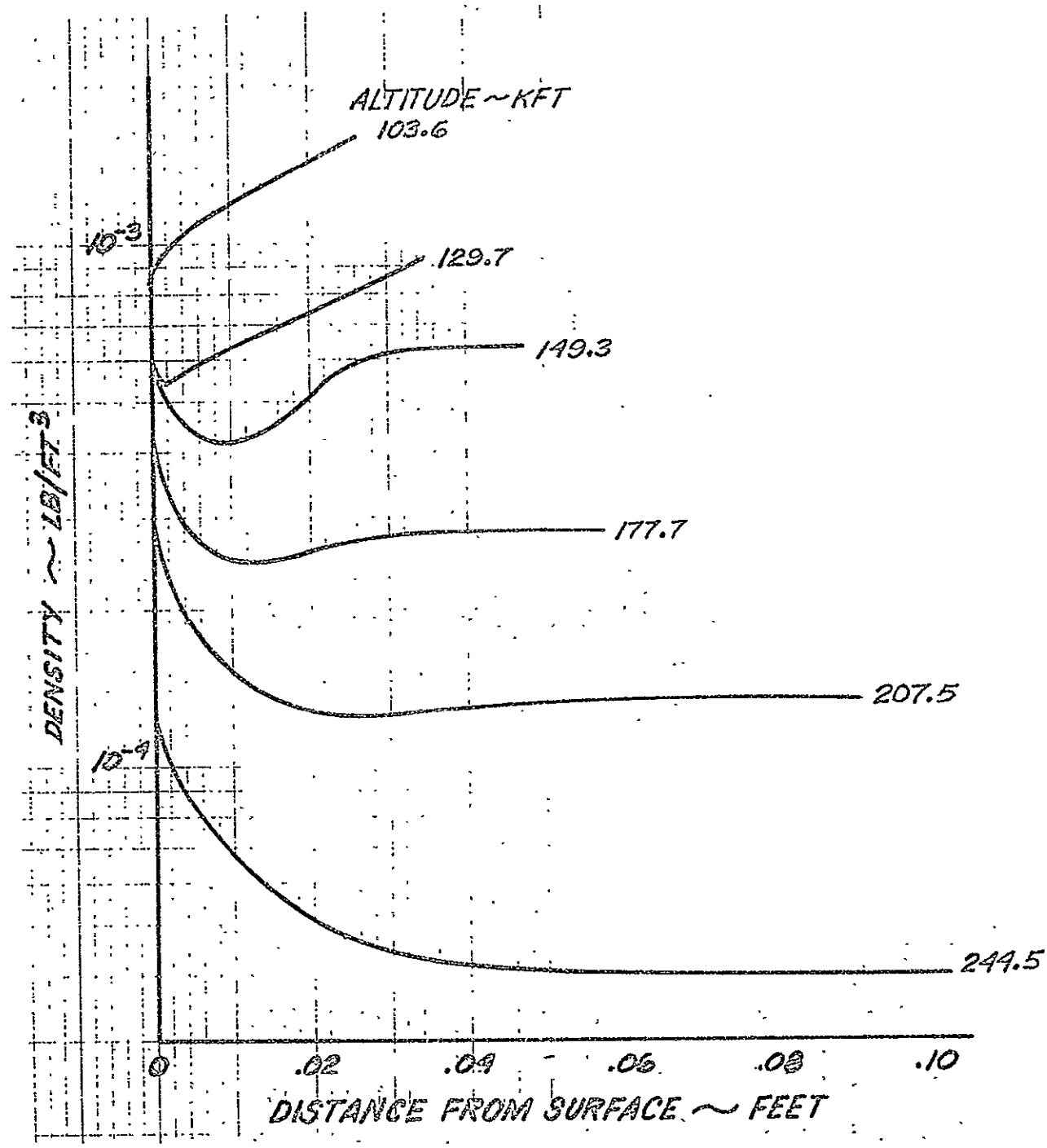

Fig. A-14 Boundary Layer Density Profile Along Leading Edge

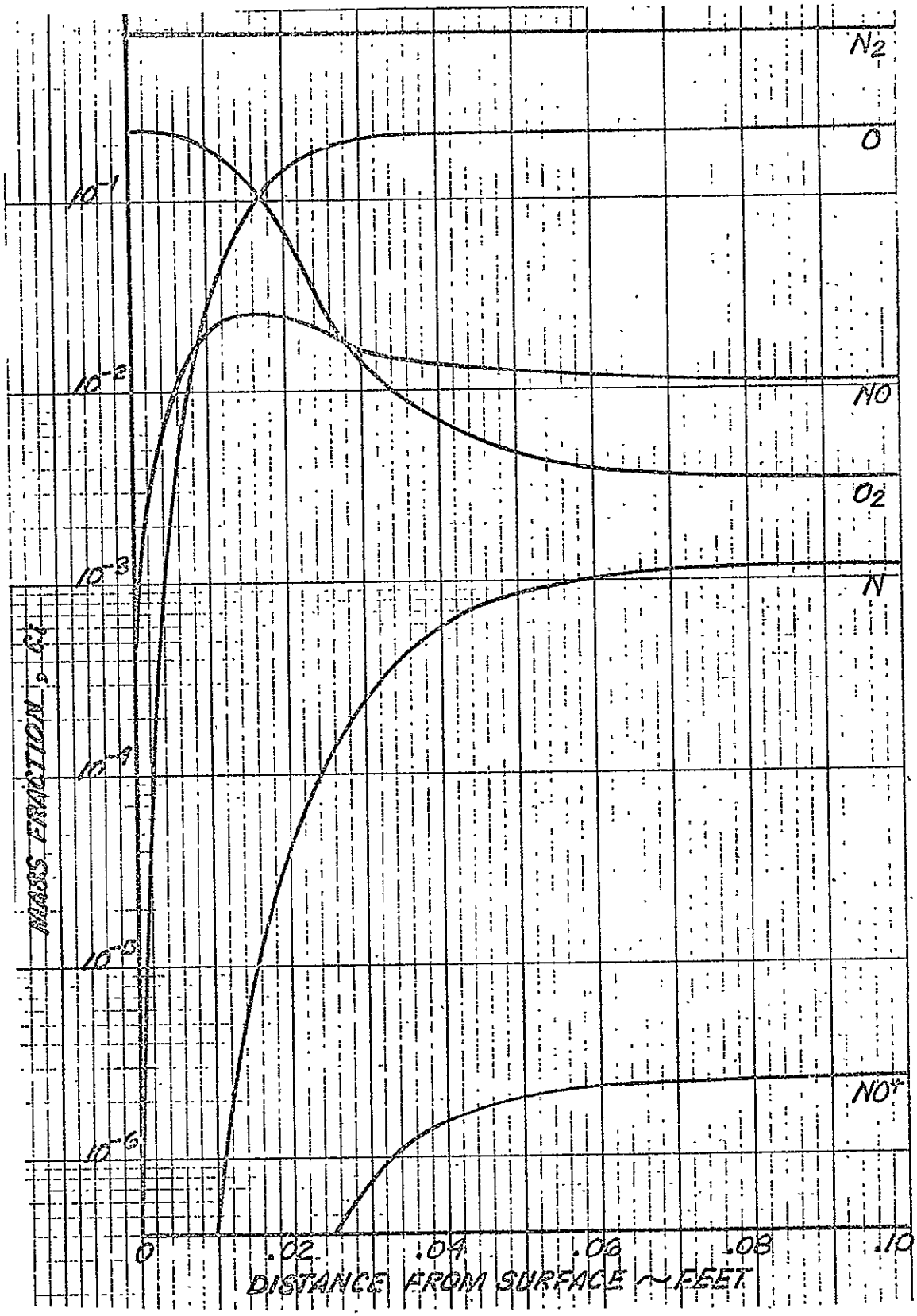

Fig. A-15 Equilibrium Air Species Concentration Profile Along Leading Edge for 244.5 kft Altitude

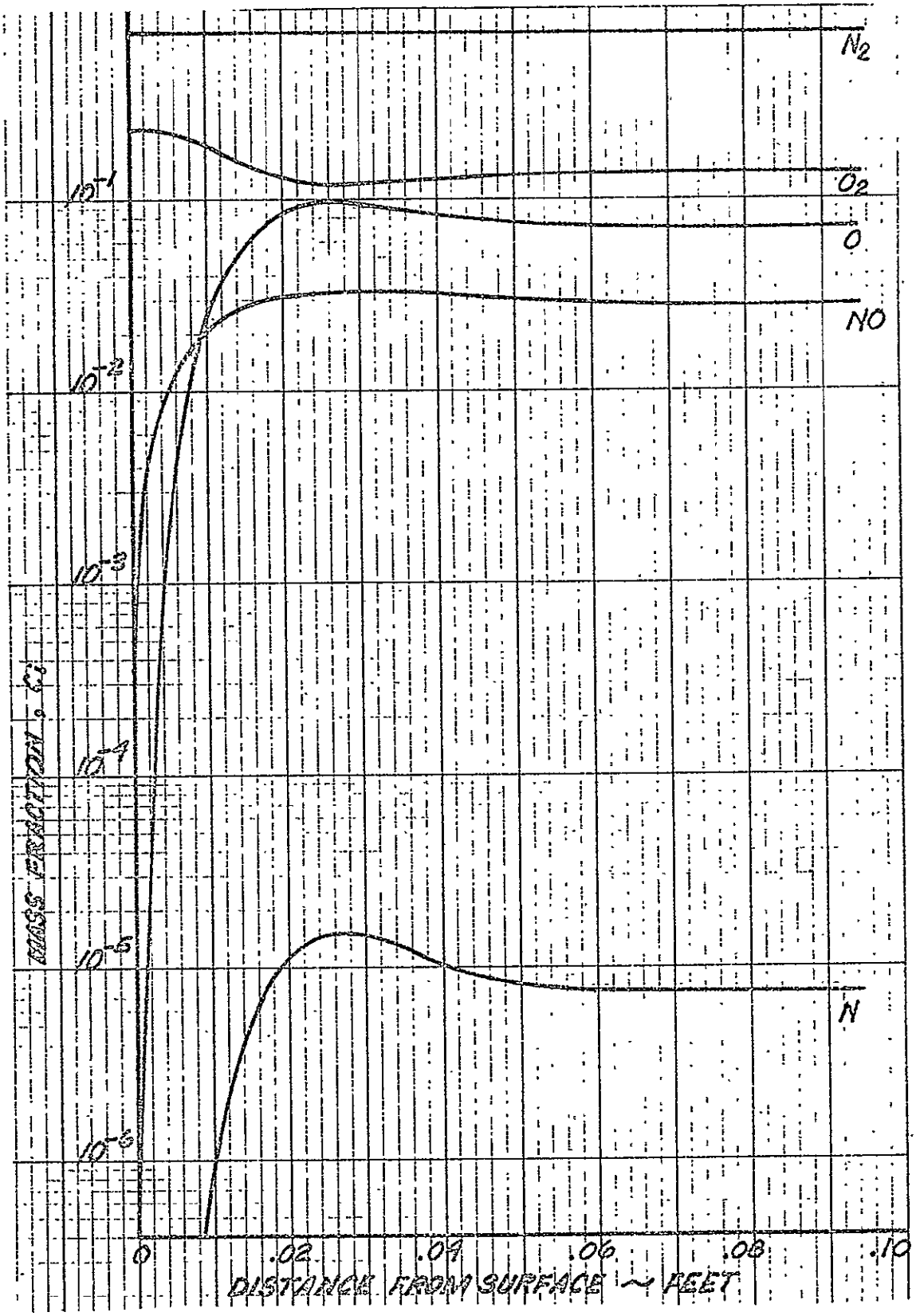

Fig. A-16 Equilibrium Air Species Concentration Profile Along Leading Edge for 207.5 kft Altitude .

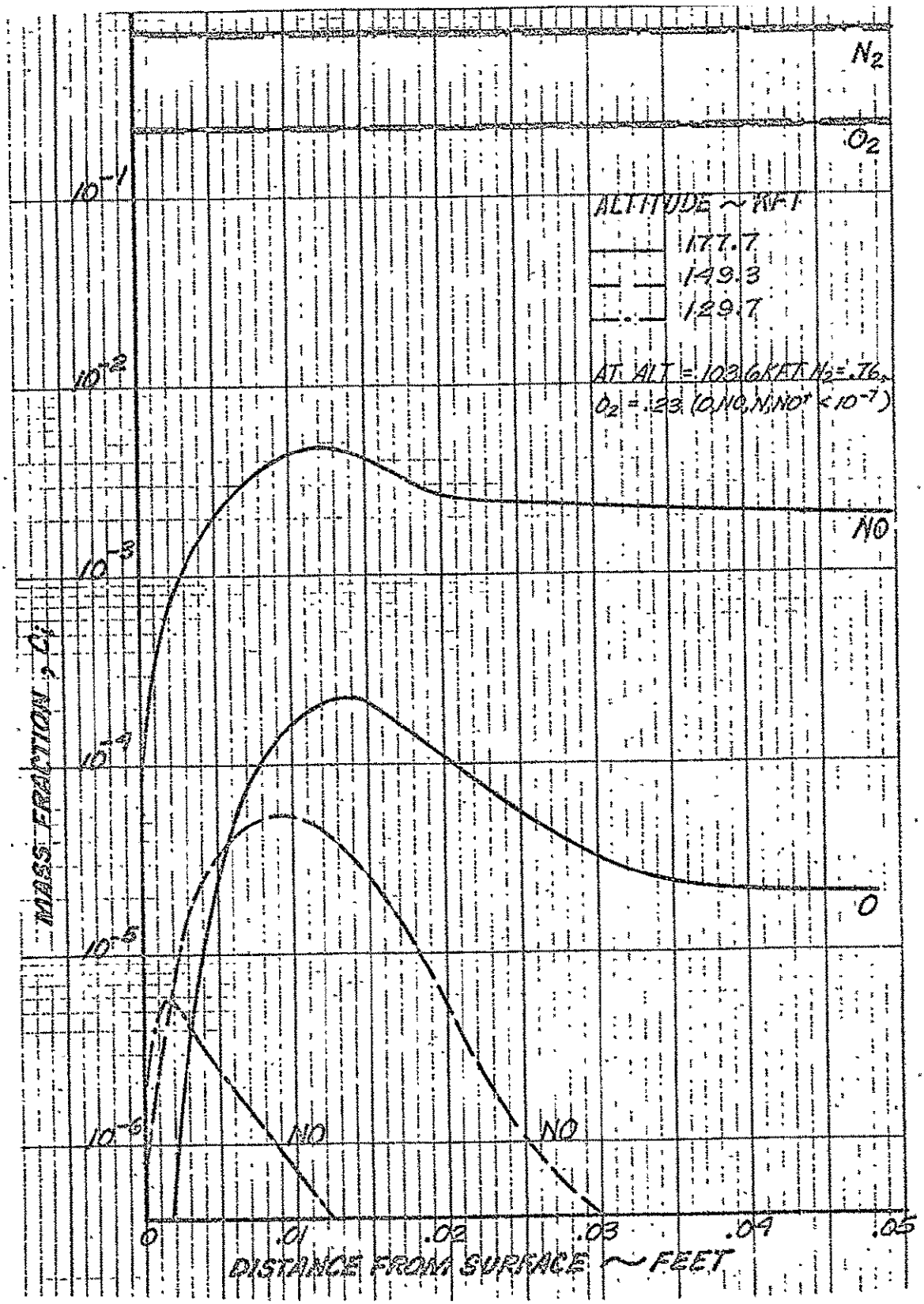

Fig. A-17 Equilibrium Air Species Concentration Profile Along Leading Edge for Three Altitudes

Appendix B

FINANCIAL STATUS REPORT

Contract Value	$90,036
Expenditures This Month	2,584
Expenditures to Date	17,575
Estimated Funds to Completion	72,461
Anticipated Over/Under Run	—
Estimated Cost of Changes Authorized but not Finalized	—
Estimated Cost of Changes Under Consideration but not Authorized	—